SIAM J. APPL. MATH.
Vol. 61, No. 2, pp. 673–700

STABILITY, BIFURCATION, AND MULTISTABILITY IN A SYSTEM OF TWO COUPLED NEURONS WITH MULTIPLE TIME DELAYS*

LESLIE P. SHAYER† AND SUE ANN CAMPBELL†‡

Abstract. A system of delay differential equations representing a model for a pair of neurons with time-delayed connections between the neurons and time delayed feedback from each neuron to itself is studied. Conditions for the linear stability of the trivial solution of this system are represented in a parameter space consisting of the sum of the time delays between the elements and the product of the strengths of the connections between the elements. It is shown that the trivial fixed point may lose stability via a pitchfork bifurcation, a Hopf bifurcation, or one of three types of codimension-two bifurcations. Multistability near these latter bifurcations is predicted using center manifold analysis and confirmed using numerical simulations.

Key words. neural network, time delay, bifurcation

AMS subject classifications. 92B20, 34K20, 34K15

PII. S0036139998344015

1. Introduction.

In 1984, Hopfield [15] considered a simplified neural network model in which each neuron is represented by a linear circuit consisting of a resistor and a capacitor and is connected to the other neurons via nonlinear sigmoidal activation functions. Assuming instantaneous updating of each neuron and communication between the neurons, Hopfield arrived at a system of first-order ordinary differential equations (ODEs). Not long afterward, Marcus and Westervelt [19] considered the effect of including discrete time delays in the connection terms to represent the propagation time between neurons and/or processing time at a given neuron. Due to the complexity of the analysis this and most subsequent work (for example, [3, 12, 28], and references therein) has focused on the situation where all connection terms in the network have the same time delay. In the work which has been done on Hopfield neural networks with multiple time delays the analysis is usually simplified by either restricting the size of the network (e.g., [20]), or considering networks with simple architectures (e.g., [1, 4, 21]). Most work which considers networks of arbitrary size with multiple time delays [11, 23, 29] has focused on establishing the global stability of fixed points.

Here we are interested in studying how time delays can affect not only the stability of fixed points of the network but also the bifurcation of new solutions when stability is lost. We thus consider a system consisting of two identical neurons, each possessing nonlinear time delayed feedback which is coupled together with nonlinear, time delayed connections. The architecture of this system is illustrated in Figure 1.

Following Hopfield's approach, each individual element is modeled as a circuit with a linear resistor and a linear capacitor. Our introduction of a nonlinear feedback term then leads to the following first-order delay differential equation (DDE):

$$\dot{x}_j(t) = -\kappa x_j(t) + \beta \tanh(x_j(t - \tau_s)). \tag{1.1}$$

*Received by the editors August 31, 1998; accepted for publication (in revised form) March 30, 1999; published electronically August 9, 2000. This research was supported by the Natural Sciences and Engineering Research Council of Canada.
http://www.siam.org/journals/siap/61-2/34401.html
†Department of Applied Mathematics, University of Waterloo, Waterloo, ON N2L 3G1, Canada.
‡Centre for Nonlinear Dynamics in Physiology and Medicine, McGill University, Montréal, QC H3A 2T5, Canada (sacampbell@uwaterloo.ca).

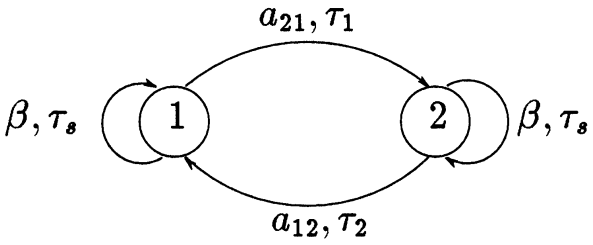

FIG. 1. *Architecture of the model.*

Here x_j represents the voltage of the neuron, κ, the ratio of the capacitance to the resistance, and β and τ_s, the feedback strength and time delay, respectively. For the model to make sense physically, κ and τ_s should be nonnegative, but β may take any value.

Equation (1.1) has been studied by many authors including Campbell [4] and Kolmanovskii and Nosov [17], who showed that the trivial solution is stable independent of the size of the delay for $-\kappa < \beta < \kappa$, but loses stability to two nontrivial equilibrium solutions for $\beta > \kappa$ and to a limit cycle for $\beta < -\kappa$ and $\tau_s > 1/\sqrt{\beta^2 - \kappa^2}\text{Arccos}(\frac{\kappa}{\beta})$. Thus by varying the parameters appropriately, this fairly simple model can reproduce two fundamental states of a neuron, quiescence and periodic firing.

Coupling two neurons of type (1.1) together with nonlinear, time-delayed connections leads to the system that we shall study

$$\begin{aligned} \dot{x}_1(t) &= -\kappa x_1(t) + \beta \tanh(x_1(t-\tau_s)) + a_{12} \tanh(x_2(t-\tau_2)), \\ \dot{x}_2(t) &= -\kappa x_2(t) + \beta \tanh(x_2(t-\tau_s)) + a_{21} \tanh(x_1(t-\tau_1)). \end{aligned} \tag{1.2}$$

We shall refer to τ_1, τ_2 as the connection time delays and a_{12}, a_{21} as the connection strengths. For the model to make sense physically, τ_1 and τ_2 should be nonnegative, but a_{12} and a_{21} are unrestricted. We shall call a particular connection or feedback excitatory when the corresponding strength is positive and inhibitory when that strength is negative. Note that a rescaling of time could be used to eliminate one parameter from (1.2) (i.e., κ could be scaled to 1, or β to ± 1). We choose not do this so that the role of these parameters in our results is apparent and so that we may consider cases when one or more of these parameters is zero.

As previously mentioned, our goal is to study the effects of the time-delayed coupling on the behavior of the system. Our choice of model allows us to study these effects when the individual neurons are in a quiescent state or a periodically firing state. Moreover, the simplicity of our model allows an in depth analysis, giving insight into possible mechanisms behind the observed behavior.

The plan for the article is as follows. In section 2, we consider the linear stability analysis of (1.2) and present some theorems about the region of stability of the trivial solution as a function of the physical parameters in the model. In section 3, we discuss the bifurcations which can occur when stability is lost and, in section 4, show how interactions between these bifurcations can lead to multistability in the system. In the final section, we will discuss the implications of our results in the context of the neural network.

2. Linear stability analysis. By inspection, we see that $(x_1, x_2) = (0, 0)$ is a fixed point of the nonlinear DDE (1.2). Linearization of (1.2) about the trivial fixed point produces the system

$$\begin{aligned} \dot{\eta}_1(t) &= -\kappa\eta_1(t) + \beta\eta_1(t-\tau_s) + a_{12}\eta_2(t-\tau_2), \\ \dot{\eta}_2(t) &= -\kappa\eta_2(t) + \beta\eta_2(t-\tau_s) + a_{21}\eta_1(t-\tau_1). \end{aligned} \tag{2.1}$$

The characteristic equation for this linear DDE is obtained by considering solutions of the form

$$\eta(t) = e^{\lambda t}\begin{pmatrix} c_1 \\ c_2 \end{pmatrix}.$$

Such solutions will be nontrivial if and only if

$$\det\begin{bmatrix} \lambda+\kappa-\beta e^{-\lambda\tau_s} & -a_{12}e^{-\lambda\tau_2} \\ -a_{21}e^{-\lambda\tau_1} & \lambda+\kappa-\beta e^{-\lambda\tau_s} \end{bmatrix} = 0.$$

Expanding the determinant, we get as the characteristic equation for system (2.1)

$$\left[(\lambda+\kappa) - \beta e^{-\lambda\tau_s}\right]^2 - a_{12}a_{21}e^{-\lambda(\tau_1+\tau_2)} = 0. \tag{2.2}$$

Defining

$$\tau = \frac{\tau_1+\tau_2}{2},$$

the characteristic equation (2.2) effectively becomes a difference of squares and may be simplified as follows.

(1) For $a_{12}a_{21} > 0$,

$$\Delta_+(\lambda)\Delta_-(\lambda) \equiv \left(\lambda+\kappa-\beta e^{-\lambda\tau_s}+\gamma e^{-\lambda\tau}\right)\left(\lambda+\kappa-\beta e^{-\lambda\tau_s}-\gamma e^{-\lambda\tau}\right) = 0, \tag{2.3}$$

where $\gamma = \sqrt{a_{12}a_{21}}$.

(2) For $a_{12}a_{21} < 0$,

$$\Delta_+(\lambda)\Delta_-(\lambda) \equiv \left(\lambda+\kappa-\beta e^{-\lambda\tau_s}+i\tilde{\gamma} e^{-\lambda\tau}\right)\left(\lambda+\kappa-\beta e^{-\lambda\tau_s}-i\tilde{\gamma} e^{-\lambda\tau}\right) = 0, \tag{2.4}$$

where $\tilde{\gamma} = \sqrt{-a_{12}a_{21}}$.

The analysis of (2.3) and (2.4) is similar, thus the majority of this section will focus on the characteristic equation (2.3). We will discuss how our results may be extended/modified for (2.4) at the end of the section.

It is well known [17, 26] that the trivial fixed point of the nonlinear DDE (1.2) is locally asymptotically stable if all the roots, λ, of the characteristic equation (2.3) satisfy $Re(\lambda) < 0$. Whether or not this is true will depend on the values of the parameters β, κ, γ, τ_s, τ. Our goal in this section is to describe the largest subset of this five-dimensional parameter space containing parameter values for which all the roots of the characteristic equation (2.3) have negative real parts. We shall refer to this subset as the *stability region* of the trivial fixed point.

Since (2.3) has a countably infinity of complex roots, it is impossible to study each one individually to determine where in the parameter space it has a negative real

part. Instead, we proceed as follows. In section 2.1 we establish various conditions on the parameters under which it can be shown that any root of (2.3) must have a negative real part. These conditions, which are given in Theorems 1 and 2, describe a subset of the full stability region. For comparison, Theorem 3 establishes a subset of parameter space which is *not* contained in the stability region. In section 2.2 we show how the subsets of Theorems 1 and 2 may be extended to give the full stability region. In particular, Theorem 4 describes the boundary of the full stability region and Theorems 5 and 6 establish how the real parts of roots of the characteristic equation (2.3) change as this boundary is crossed. Finally, Theorems 7, 8, and 9 complete the task by describing various two-dimensional slices of the five-dimensional stability region.

2.1. Subsets of the stability region. The following two theorems establish subsets of the full stability region.

THEOREM 1. *If the parameters satisfy* $0 < \gamma < \kappa - |\beta|$, $\tau_s \geq 0$, *and* $\tau \geq 0$, *then all the roots of the characteristic equation* (2.3) *have negative real parts.*

Proof. Consider the characteristic function of (2.3), rewritten in the more compact form

$$\Delta_{\pm}(\lambda) = \lambda + \kappa - \beta e^{-\lambda\tau_s} \pm \gamma e^{-\lambda\tau}.$$

Let $\lambda = \mu + i\omega$, $\mu, \omega \in \mathbb{R}$ and separate into real and imaginary parts to obtain $\Delta_{\pm}(\lambda) = R_{\pm}(\mu,\omega) + iI_{\pm}(\mu,\omega)$, where

$$R_{\pm}(\mu,\omega) = \mu + \kappa - \beta e^{-\mu\tau_s}\cos(\omega\tau_s) \pm \gamma e^{-\mu\tau}\cos(\omega\tau) \tag{2.5}$$

and

$$I_{\pm}(\mu,\omega) = \omega + \beta e^{-\mu\tau_s}\sin(\omega\tau_s) \mp \gamma e^{-\mu\tau}\sin(\omega\tau). \tag{2.6}$$

From (2.5), we see that

$$R_{\pm}(\mu,\omega) \geq \mu + \kappa - |\beta| e^{-\mu\tau_s} - \gamma e^{-\mu\tau}. \tag{2.7}$$

Denote the right-hand side of (2.7) by $R_1(\mu)$. Clearly,

$$R_1(0) = \kappa - |\beta| - \gamma > 0$$

under the assumptions of the theorem. Furthermore,

$$R_1'(\mu) = 1 + |\beta|\tau_s e^{-\mu\tau_s} + \tau\gamma e^{-\mu\tau} > 0.$$

Hence, $R_1(\mu) > 0$ for all $\mu \geq 0$ and $R_{\pm}(\mu,\omega) > 0$ for all $\mu \geq 0, \omega \in \mathbb{R}$.

Now let $\lambda = \mu + i\omega$ be an arbitrary root of the characteristic equation (2.3). Then μ and ω must satisfy $R_+(\mu,\omega) = 0$ and $I_+(\mu,\omega) = 0$ or $R_-(\mu,\omega) = 0$ and $I_-(\mu,\omega) = 0$. But from the discussion above this implies $\mu < 0$. Thus all the roots of the characteristic equation have negative real parts. ∎

THEOREM 2. *If the parameters satisfy* $0 \leq \kappa < -\beta$, $0 < \gamma < -\beta$, $0 \leq \tau_s < -\frac{1}{2\beta}$ *and* $\tau \geq 0$, *then all the roots of the characteristic equation* (2.3) *have negative real part.*

Proof. To begin, let $\lambda = \mu + i\omega$ in (2.3). Separating into real and imaginary parts, we obtain

$$\mu = -\kappa + \beta e^{-\mu\tau_s}\cos(\omega\tau_s) \mp \gamma e^{-\mu\tau}\cos(\omega\tau) \tag{2.8}$$

and

$$\omega = -\beta e^{-\mu\tau_s}\sin(\omega\tau_s) \pm \gamma e^{-\mu\tau}\sin(\omega\tau). \tag{2.9}$$

We now assume that (2.8) and (2.9) have roots μ and ω, where $\omega \geq 0$ (without loss of generality since complex roots of (2.3) come in complex conjugate pairs). From (2.9), using the conditions imposed on γ, we find that $\omega < -2\beta$. The condition $0 \leq \tau_s < -\frac{1}{2\beta}$ then implies that $0 \leq \omega\tau_s < 1$. Hence, $1/2 < \cos(1) < \cos(\omega\tau_s) \leq 1$ and $0 \leq \sin(\omega\tau_s) < \sin(1) < 1$.

Isolating the last term in both (2.8) and (2.9), squaring and adding, we obtain the necessary condition

$$(\mu+\kappa)^2 + \omega^2 - 2\beta e^{-\mu\tau_s}\left\{(\mu+\kappa)\cos(\omega\tau_s) - \omega\sin(\omega\tau_s)\right\} + \beta^2 e^{-2\mu\tau_s} - \gamma^2 e^{-2\mu\tau} = 0, \tag{2.10}$$

for a solution of (2.8) and (2.9) to exist. For fixed values of κ, ω, τ_s, and τ, we call the left-hand side of (2.10) $M(\mu)$ and note that

$$M(0) = \kappa^2 - 2\beta\kappa\cos(\omega\tau_s) + \beta^2 + \omega^2 + 2\beta\omega\sin(\omega\tau_s) - \gamma^2.$$

Since $\sin(\omega\tau_s) < \omega\tau_s$ and $\tau_s < -\frac{1}{2\beta}$, then

$$\omega^2 + 2\beta\omega\sin(\omega\tau_s) \geq \omega^2(1 + 2\beta\tau_s) > 0,$$

which, recalling that $\beta < 0$, $\cos(\omega\tau_s) > 0$ and $\gamma^2 < \beta^2$, yields $M(0) > 0$. Taking the derivative of $M(\mu)$ with respect to μ, we obtain

$$\begin{aligned}\frac{dM}{d\mu} = 2\big\{&\tau\gamma^2 e^{-2\mu\tau} - \beta\omega\tau_s e^{-\mu\tau_s}\sin(\omega\tau_s) + (\mu+\kappa)\left[1 + \beta\tau_s e^{-\mu\tau_s}\cos(\omega\tau_s)\right] \\ &- \beta e^{-\mu\tau_s}\left[\cos(\omega\tau_s) + \beta\tau_s e^{-\mu\tau_s}\right]\big\}.\end{aligned} \tag{2.11}$$

Since $\beta < 0$, $\omega \geq 0$, $\gamma > 0$, $\tau_s \geq 0$,$\tau \geq 0$, $\kappa \geq 0$, $\mu \geq 0$, $\sin(\omega\tau_s) \geq 0$, and $\cos(\omega\tau_s) > 0$, the first two terms in the first line of expression (2.11) are nonnegative. We now consider the other two in turn.

(1) From $0 \leq \tau_s < -\frac{1}{2\beta}$ and $\mu \geq 0$, we have $0 < e^{-\mu\tau_s} \leq 1$. Combining this with $\cos(\omega\tau_s) \leq 1$, we get

$$(\mu+\kappa)\left[1 + \beta\tau_s e^{-\mu\tau_s}\cos(\omega\tau_s)\right] > (\mu+\kappa)\left(1 - \frac{1}{2}\right) \geq 0.$$

(2) From $\beta < 0$, $\frac{1}{2} < \cos(1) < \cos(\omega\tau_s)$, $\tau_s < -\frac{1}{2\beta}$, and $0 < e^{-\mu\tau_s} \leq 1$,

$$-\beta e^{-\mu\tau_s}\left[\cos(\omega\tau_s) + \beta\tau_s e^{-\mu\tau_s}\right] > -\beta e^{-\mu\tau_s}\left(\cos(1) - \frac{1}{2}\right) > 0.$$

Thus, $\frac{dM}{d\mu} > 0$ for $\mu \geq 0$. Since $M(0) > 0$, we conclude that $M(\mu) > 0$ if $\mu \geq 0$. Thus if $M(\mu) = 0$, then $\mu < 0$; i.e., all roots of the characteristic equation have negative real part. □

The following theorem shows that parameter values analogous to those of Theorem 2, but with $\beta > 0$, do not lie inside the region of stability, i.e., the trivial fixed point is unstable for these parameter values.

THEOREM 3. *If $0 \le \kappa < \beta$, then the characteristic equation* (2.3) *has a root with a positive real part for all values of $\gamma \ge 0$, $\tau_s \ge 0$, and $\tau \ge 0$.*

Proof. Recall from the characteristic equation (2.3), that $\Delta_-(\lambda) = \lambda + \kappa - \beta e^{-\lambda\tau_s} - \gamma e^{-\lambda\tau}$. Then, under the assumption of the theorem,

$$\Delta_-(0) = \kappa - \beta - \gamma < 0$$

and

$$\lim_{\lambda\to+\infty} \Delta_-(\lambda) = \lim_{\lambda\to+\infty} [\lambda + \kappa - \beta e^{-\lambda\tau_s} - \gamma e^{-\lambda\tau}] = +\infty$$

for all $\gamma \ge 0$, $\tau_s \ge 0$, and $\tau \ge 0$. Hence, as $\Delta_-(\lambda)$ is a continuous function of λ, there exists a $\lambda^* > 0$ such that $\Delta_-(\lambda^*) = 0$ for any fixed values of $\tau_s \ge 0$, $\tau \ge 0$, $\gamma \ge 0$, and $\kappa < \beta$. Thus, the characteristic equation has a positive real root for these parameter values. □

2.2. Full stability region. The next theorem helps to determine the full stability region of the trivial fixed point by describing its boundary in parameter space.

THEOREM 4. *Consider the trivial fixed point of the DDE* (1.2). *As β, κ, γ, τ_s, and τ vary in parameter space, the number of eigenvalues with* $\mathrm{Re}(\lambda) > 0$, *counting multiplicities, can change only if an eigenvalue passes through the imaginary axis in the complex plane.*

Proof. See Bélair and Campbell [2, Lemma 2.1], with $m = 3$, $a_1 = \kappa$, $\tau_1 = 0$, $a_2 = \beta$, $\tau_2 = \tau_s$, $a_3 = \mp\gamma$, and $\tau_3 = \tau$. □

Theorem 4 implies that the subsets of parameter space defined by the equations $\lambda = 0$ (i.e., (2.3) has a zero root) and $\lambda = i\omega$ (i.e., (2.3) has a pair of pure imaginary roots) form the boundary of the stability region. The next step is thus to describe these subsets.

The case $\lambda = 0$ is simple. Substituting $\lambda = 0$ into the characteristic equation (2.3), we get the restriction

$$(\kappa - \beta + \gamma)(\kappa - \beta - \gamma) = 0.$$

The second term is zero when

$$\gamma = \gamma_0 \stackrel{\text{def}}{=} \kappa - \beta, \qquad \kappa > \beta, \qquad \beta \in \mathbb{R}, \tag{2.12}$$

corresponding to the $\Delta_-(\lambda)$ having a zero root. The first term is zero when

$$\gamma = -\gamma_0 = \beta - \kappa, \qquad 0 \le \kappa < \beta, \tag{2.13}$$

corresponding to $\Delta_+(\lambda)$ having a zero root. Note that from Theorem 3, this subset cannot form part of the boundary of the stability region.

The case $\lambda = i\omega$ is more complicated. Substituting $\lambda = i\omega$ into (2.3) and separating into real and imaginary parts, we obtain the following equations:

$$\kappa - \beta\cos(\omega\tau_s) = \pm\gamma\cos(\omega\tau) \tag{2.14}$$

and

$$-\omega - \beta\sin(\omega\tau_s) = \pm\gamma\sin(\omega\tau). \tag{2.15}$$

In principle, we can eliminate ω from these equations, obtaining a single equation in β, κ, γ, τ, and τ_s, which will define a hypersurface in the parameter space. Since

this cannot be carried out in practice, in order to describe this hypersurface, we consider its intersection with the space $\kappa =$ constant $\beta =$ constant and $\tau_s =$ constant, which we can represent in parametric form with γ and τ as functions of ω.

First, we find γ by squaring and adding (2.14) and (2.15):

$$\gamma = \gamma_H(\omega) \stackrel{\text{def}}{=} \sqrt{\kappa^2 + \beta^2 + \omega^2 - 2\beta\kappa\cos(\omega\tau_s) + 2\beta\omega\sin(\omega\tau_s)}. \tag{2.16}$$

Taking the ratio of (2.14) and (2.15) and solving for τ yields an expression involving the inverse tangent function. Noting that the sign of $\cos(\omega\tau)$ may be obtained from (2.14), we find that the appropriate expression for τ is

(2.17)
$$\tau = \tau_j^{\pm}(\omega) \stackrel{\text{def}}{=} \begin{cases} \frac{1}{\omega}[\text{Arctan}\left(\frac{-\omega-\beta\sin(\omega\tau_s)}{\kappa-\beta\cos(\omega\tau_s)}\right) + 2j\pi] & \text{if} \pm(\kappa - \beta\cos(\omega\tau_s)) > 0, \\ \frac{1}{\omega}[\text{Arctan}\left(\frac{-\omega-\beta\sin(\omega\tau_s)}{\kappa-\beta\cos(\omega\tau_s)}\right) + (2j+1)\pi] & \text{if} \pm(\kappa - \beta\cos(\omega\tau_s)) < 0 \end{cases}$$

for $j = 0, 1, \ldots$, where $\text{Arctan}(u)$ is the principal branch of the inverse tangent function. A detailed analysis of how τ switches between branches as ω varies, for fixed values of κ, β, and τ_s, may be found in [25, Appendix A]. Clearly, equations (2.17) represent an infinite family of curves. We note the following limits, which hold for all values of κ and τ_s:

$$\lim_{\omega\to 0^+} \gamma_H = |\kappa - \beta|, \qquad \lim_{\omega\to+\infty} \gamma_H = +\infty, \tag{2.18}$$

$$\lim_{\omega\to 0^+} \tau_j^{\pm} = \begin{cases} \frac{\beta\tau_s+1}{\beta-\kappa} \stackrel{\text{def}}{=} \tau^* & \text{if } j = 0, \\ +\infty & \text{otherwise,} \end{cases} \qquad \lim_{\omega\to+\infty} \tau_j^{\pm} = 0. \tag{2.19}$$

The finite limit in the first part of (2.19) may be established by performing a Taylor expansion in (2.17). This value is in the parameter space only if $0 \le \kappa < \beta$ or $\beta < 0 \le \kappa$ and $\tau_s \ge -\frac{1}{\beta} \stackrel{\text{def}}{=} \tau_s^*$. We shall refer to the branch of (2.17) that corresponds to the finite limit as the *exceptional branch*.

Remark. If $\kappa > |\beta|$, then the "+" sign in (2.17) is associated with the ">" sign in (2.17) and similarly, the "−" sign with the "<" sign.

In summary, we have shown that

(1) the lines, $\gamma = \pm\gamma_0$, with τ and τ_s positive and arbitrary, represent the set of points in parameter space for which the trivial fixed point of the DDE (1.2) has a zero eigenvalue;
(2) the curve (with multiple branches) defined by (2.16) and (2.17) represents the set of points in parameter space for which the trivial fixed point of the DDE (1.2) has a pair of purely imaginary eigenvalues.

We shall refer to the lines $\gamma = \pm\gamma_0$, (i.e., (2.12) or (2.13)) in the $\gamma\tau$-plane as the $\lambda = 0$ *lines*, and the curve defined by (2.16) and (2.17) as the $\lambda = i\omega$ *curve*.

We now present two theorems which describe how the real parts of the roots of (2.3) change as a $\lambda = 0$ line or the $\lambda = i\omega$ curve is crossed in the $\gamma\tau$-plane.

THEOREM 5. *Consider crossing a $\lambda = 0$ line, while moving along a line $\tau =$* constant *in the $\gamma\tau$-plane in the direction of increasing γ. Then the number of roots λ of the characteristic equation* (2.3) *with* $\text{Re}(\lambda) > 0$ *increases by* 1, *unless $\tau < \tau^*$ in which case it decreases by* 1.

Proof. Recall that the $\lambda = 0$ lines are defined by the zero roots of $\Delta_\pm(\lambda) = 0$, i.e.,

$$\lambda + \kappa - \beta e^{-\lambda\tau_s} \pm \gamma e^{-\lambda\tau} = 0.$$

Differentiating with respect to γ, we obtain

$$\frac{d\lambda}{d\gamma} = \frac{\mp e^{-\lambda\tau}}{1 + \beta\tau_s e^{-\lambda\tau_s} \mp \gamma\tau e^{-\lambda\tau}}.$$

If $\lambda = 0$ is a root of $\Delta_\pm(\lambda) = 0$, then $\gamma = \pm\gamma_0 = \mp(\kappa - \beta)$ and the derivative becomes

$$\left.\frac{d\lambda}{d\gamma}\right|_{\lambda=0,\gamma=\mp\gamma_0} = \frac{\mp 1}{(\kappa-\beta)\tau + (1+\beta\tau_s)}.$$

Hence, $\frac{d\lambda}{d\gamma}\,|_{\lambda=0} \gtrless 0$ if and only if

$$\tau \lessgtr \frac{\beta\tau_s + 1}{\beta - \kappa}. \qquad \square$$

THEOREM 6. *Consider moving along a line* $\tau =$ constant *in the* $\gamma\tau$*-plane in the direction of increasing* γ*. If this line cuts a branch of the* $\lambda = i\omega$ *curve along which* $\tau_j^\pm$ *is a decreasing (increasing) function of* ω*, then as this branch is crossed, the number of roots* λ *of the characteristic equation* (2.3) *with* $\mathrm{Re}(\lambda) > 0$ *increases (decreases) by* 2.

Proof. The $\lambda = i\omega$ curve defined by (2.16) and (2.17) gives the points in the $\gamma\tau$-plane, where the real part of λ is zero. We can now prove our claim by considering the appropriate derivatives. Differentiating equation (2.17), with respect to ω, we get

$$\frac{d\tau_j^\pm}{d\omega} = \frac{-1}{\gamma_H^2\omega}\left[\tau_j^\pm\gamma_H^2 + \kappa + \beta[\kappa\tau_s - 1]\cos(\omega\tau_s) - \beta\omega\tau_s\sin(\omega\tau_s) - \beta^2\tau_s\right]. \tag{2.20}$$

Implicit differentiation of (2.3) with respect to γ and substitution of $\lambda = i\omega$ leads to the following expression for the real part of $\frac{d\lambda}{d\gamma}$:

$$\left.\frac{d\mathrm{Re}\lambda}{d\gamma}\right|_{\lambda=i\omega} = \frac{\tau_j^\pm\gamma_H^2 + \kappa + \beta[\kappa\tau_s - 1]\cos(\omega\tau_s) - \beta\omega\tau_s\sin(\omega\tau_s) - \beta^2\tau_s}{\gamma_H\left\{\left[1 + \beta\tau_s\cos(\omega\tau_s) \pm \gamma_H\tau_j^\pm\cos(\omega\tau_j^\pm)\right]^2 + \left[-\beta\tau_s\sin(\omega\tau_s) \mp \gamma_H\tau_j^\pm\sin(\omega\tau_j^\pm)\right]^2\right\}}.$$

By inspection, we see that the above denominator is always nonnegative. By (2.20), $\frac{d\tau_j^\pm}{d\omega} < 0$ implies that $\frac{d\mathrm{Re}\lambda}{d\gamma} > 0$. Thus, the real part of λ becomes positive when $\tau_j^\pm$ is a decreasing function of ω and the characteristic equation (2.3) gains a pair of roots with positive real part. Similarly, if $\frac{d\tau_j^\pm}{d\omega} > 0$, then the real part of λ becomes negative, which completes the proof. $\square$

Let us summarize our results so far. Theorems 1 and 2 establish regions in parameter space which form subsets of the stability region of the trivial fixed point of (1.2). Theorem 4 shows that the full stability region for fixed κ, τ_s, and β may be obtained from these subsets by increasing γ until one reaches the $\lambda = 0$ lines, i.e.,

(2.12) or (2.13), or the $\lambda = i\omega$ curve, defined by (2.16) and (2.17). Theorems 5 and 6 describe how the real parts of the roots of the characteristic equation change as the boundary of the stability region is crossed.

The rest of this subsection is concerned with explicitly describing the full stability region. To do this, one needs to understand the relative positions of the $\lambda = 0$ lines and the $\lambda = i\omega$ curve in the $\gamma\tau$-plane for fixed κ, τ_s, and β. This is the subject of the next two lemmas.

LEMMA 1. *If $\kappa > |\beta|$, then the $\lambda = i\omega$ curve is bounded on the left by the line $\gamma = \kappa - |\beta|$.*

Proof. From (2.14), which holds along $\gamma = \gamma_H$, we have

$$\gamma_H \geq \pm\gamma_H \cos(\omega\tau) = \kappa - \beta\cos(\omega\tau_s) \geq \kappa - |\beta|,$$

which establishes the result. □

LEMMA 2. *The $\lambda = i\omega$ curve has the property that γ_H is monotone increasing as a function of ω and satisfies $\gamma_H > |\kappa - \beta|$ for all $\omega > 0$ if τ_s satisfies*

$$0 \leq \tau_s \leq \frac{-1 + \sqrt{1 + \frac{\kappa}{|\beta|}}}{\kappa}.$$

When $\beta < 0$, the converse is also true.

Proof. Differentiating (2.16) with respect to ω, we obtain

$$\frac{d\gamma_H}{d\omega} = \frac{1}{\gamma_H}[\omega + \beta(1 + \kappa\tau_s)\sin(\omega\tau_s) + \beta\omega\tau_s\cos(\omega\tau_s)]. \tag{2.21}$$

For $\tau_s = 0$ and $\omega > 0$, $\frac{d\gamma_H}{d\omega} = \frac{\omega}{\gamma_H} > 0$. For $\omega\tau_s > 0$, $\beta\cos(\omega\tau_s) \geq -|\beta|$ and $\beta\sin(\omega\tau_s) > -|\beta|\omega\tau_s$; hence

$$\begin{aligned}\frac{d\gamma_H}{d\omega} &> \frac{\omega}{\gamma_H}(1 - 2|\beta|\tau_s - \kappa|\beta|\tau_s^2) \\ &= \frac{\omega|\beta|}{\gamma_H\kappa}\left[\frac{\kappa}{|\beta|} + 1 - (\kappa\tau_s + 1)^2\right] \\ &\geq 0\end{aligned}$$

for $\tau_s \leq \frac{-1+\sqrt{1+\kappa/|\beta|}}{\kappa}$. It now follows from the first limit in (2.18), that $\gamma_H > |\kappa - \beta|$ for all $\omega > 0$.

To prove the converse, consider the Taylor expansion of $\frac{d\gamma_H}{d\omega}$ about $\omega = 0$:

$$\begin{aligned}\frac{d\gamma_H}{d\omega} = \omega&\left\{\frac{1 + 2\beta\tau_s + \beta\kappa\tau_s^2}{|\kappa - \beta|}\right\} \\ &-\frac{1}{2|\kappa - \beta|}\omega^3\left\{\frac{\beta\tau_s^3}{3}(4 + \kappa\tau_s) + \frac{(1 + 2\beta\tau_s + \beta\kappa\tau_s^2)^2}{(\kappa - \beta)^2}\right\} + O(\omega^5).\end{aligned}$$

If $\tau_s > \frac{-1+\sqrt{1+\frac{\kappa}{|\beta|}}}{\kappa}$ and $\beta < 0$, then the first term of this expression is negative, and hence $\gamma_H(\omega)$ is decreasing for ω sufficiently close to zero. □

Remark. We denote this special value $\tau_s = \frac{-1+\sqrt{1+\frac{\kappa}{|\beta|}}}{\kappa}$ by its equivalent form

$$\tau_s^{(1)} = \frac{1}{\left(1 + \sqrt{1 + \frac{\kappa}{|\beta|}}\right)|\beta|}, \tag{2.22}$$

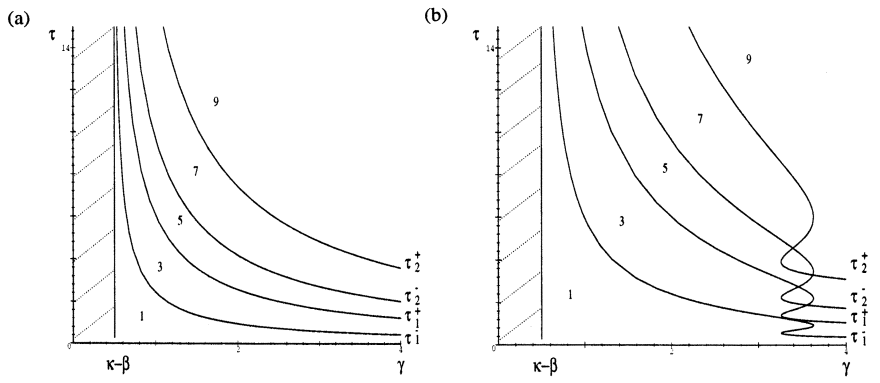

FIG. 2. *Diagram of the $\lambda = 0$ line and the branches of the $\lambda = i\omega$ curve for $0 < \beta < \kappa$ (shown here, $\beta = 1$, $\kappa = 3/2$).* (a) $0 \le \tau_s \le \tau_s^{(1)}$ *($\tau_s = 0.01$).* (b) $\tau_s > \tau_s^{(1)}$ *($\tau_s = 1.2$). The stability region in each diagram is shaded, and the number of roots with positive real parts in other regions is as indicated.*

and refer to it as the *first transition point.* Note that $\tau_s^{(1)} \le \tau_s^*$. Furthermore, Lemma 2 also applies to $\kappa = 0$, in which case $\tau_s^{(1)} = \frac{1}{2|\beta|}$.

We now have the background to discuss the stability region when $|\beta| < \kappa$, which is the subject of the next two theorems.

THEOREM 7. *For any fixed values of β, κ, and τ_s, satisfying $0 < \beta < \kappa$ and $\tau_s \ge 0$, the stability region of the trivial fixed point of the nonlinear DDE* (1.2) *is the vertical strip $0 < \gamma < \kappa - \beta$, $\tau \ge 0$.*

Proof. By Theorem 1, $0 < \gamma < \kappa - |\beta|$, all roots, λ, of the characteristic equation satisfy $\mathrm{Re}(\lambda) < 0$ for all values of $\tau \ge 0$ and $\tau_s \ge 0$. Furthermore, from Lemma 1, we know that the $\lambda = i\omega$ curve always lies to the right of the line $\gamma = \kappa - |\beta|$. If $\beta > 0$, this line coincides with the $\lambda = 0$ line, $\gamma = \kappa - \beta$, thus the boundary of the stability region is always this line. □

This Theorem is illustrated in Figure 2.

Now consider the case when $0 < -\beta < \kappa$. From (2.18) we see that $\lim_{\omega \to 0} \gamma_H(\omega) = \kappa - \beta$ and from Lemma 1 that the minimum value γ_H can achieve is $\kappa - |\beta|$. Further, the proof of Lemma 2 shows that for $\tau_s > \tau_s^{(1)}$, $\gamma_H(\omega)$ is decreasing for $\omega > 0$ sufficiently small. It follows that the branches of the $\lambda = i\omega$ curve cross $\gamma = \kappa - \beta$ (i.e., the $\lambda = 0$ line) and γ_H attains a minimum value $\gamma_{\min}$ (which depends on κ and τ_s), satisfying $\kappa - |\beta| \le \gamma_{\min} < \kappa - \beta$. Clearly $\gamma_{\min} = \gamma_H(\omega_{\min})$, where $\omega_{\min} \ne 0$ satisfies

$$\left.\frac{d\gamma_H}{d\omega}\right|_{\omega = \omega_{\min}} = 0.$$

Define the associated τ values by $\tau_{j,\min}^{\pm} = \tau_j^{\pm}(\omega_{\min})$. We can now state our second stability theorem.

THEOREM 8. *Let β, κ, and τ_s be fixed with $0 < -\beta < \kappa$ and let $\tau_j^{\pm}$ be as defined in* (2.17)*. Then we have the following.*

(1) *For $0 \le \tau_s < \tau_s^{(1)}$, the stability region is the vertical strip $0 < \gamma < \kappa - \beta$, $\tau \ge 0$.*

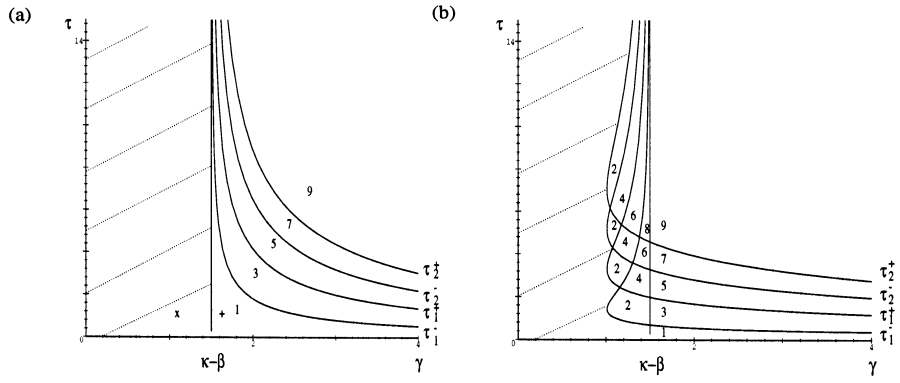

FIG. 3. *Diagram of the $\lambda = 0$ line and the branches of the $\lambda = i\omega$ curve for $0 \le \kappa < -\beta$ (shown here, $\beta = -1$, $\kappa = 1/2$).* (a) $0 \le \tau_s < \tau_s^{(1)}$ *($\tau_s = 0.01$).* (b) $\tau_s^{(1)} \le \tau_s \le \tau_s^*$ *($\tau_s = 0.8$). The stability region in both diagrams is shaded, and the number of roots with positive real parts in other regions is as indicated.*

(2) *For $\tau_s^{(1)} \le \tau_s \le \tau_s^*$, the stability region is the set of points (γ, τ), satisfying*
   (a) $0 < \gamma < \gamma_{\min}$, $\tau \ge 0$;
   (b) $\gamma_{\min} < \gamma < \kappa - \beta$,
      (i) $0 < \tau < \tau_1^- \le \tau_{1,\min}^-$;
      (ii) $\tau_{j,\min}^- \le \tau_j^- < \tau < \tau_j^+ \le \tau_{j,\min}^+$; *and*
      (iii) $\tau_{j,\min}^+ \le \tau_j^+ < \tau < \tau_{j+1}^- \le \tau_{j+1,\min}^-$
      for $j = 1, 2, \ldots$.

(3) *For $\tau_s > \tau_s^*$, the stability region is the set of points (γ, τ), satisfying*
   (a) $0 < \gamma < \gamma_{\min}$, $\tau \ge 0$, $\gamma_{\min} \to \kappa - |\beta|$ *as* $\tau_s \to \infty$;
   (b) $\gamma_{\min} < \gamma < \kappa - \beta$,
      (i) $\max(\tau_0^+, 0) < \tau < \tau_1^- \le \tau_{1,\min}^-$;
      (ii) $\tau_{j,\min}^- \le \tau_j^- < \tau < \tau_j^+ \le \tau_{j,\min}^+$; *and*
      (iii) $\tau_{j,\min}^+ \le \tau_j^+ < \tau < \tau_{j+1}^- \le \tau_{j+1,\min}^-$
      for $j = 1, 2, \ldots$.

Proof. By Theorem 1, for $\kappa > |\beta|$ and $\gamma < \kappa - |\beta|$, all roots of the characteristic equation (2.3) λ satisfy $\mathrm{Re}(\lambda) < 0$. Moreover, Theorem 4 extends the subset of the stability region to the boundary $\mathrm{Re}(\lambda) = 0$.

For $0 \le \tau_s < \tau_s^{(1)}$, Lemma 2 implies that the boundary is the $\lambda = 0$ line, $\gamma = \kappa - \beta$. This establishes statement 1.

As discussed above, for $\tau_s \ge \tau_s^{(1)}$, some portion of the $\lambda = i\omega$ curve lies to the left of the $\lambda = 0$ line $\gamma = \kappa - \beta$, hence the boundary of the stability region must be composed of parts of the $\lambda = i\omega$ curve and parts of this line.

Consider the region R_j^- defined by

$$R_j^- = \left\{ (\gamma, \tau) : \gamma_{\min} \le \gamma \le \kappa - \beta, \quad \tau_{j,\min}^- \le \tau \le \tau_{j,\min}^+ \right\}.$$

It can be shown that the curve $\{(\gamma_H(\omega_1), \tau_j^-(\omega_1)) : 0 \le \omega_1 \le \omega_{\min}\}$ defines a curve $\{(\gamma_H, \tau_j^-(\gamma_H)) : \gamma_{\min} \le \gamma_H \le \kappa - \beta\}$ with τ_j^- a continuous, increasing func-

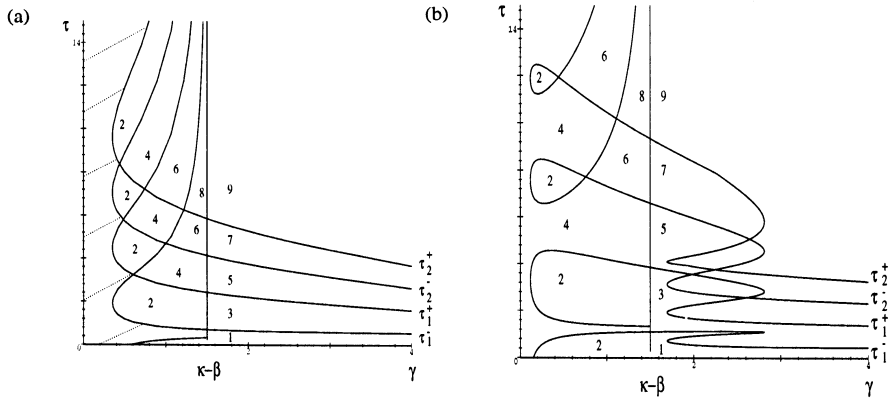

FIG. 4. *Diagram of the $\lambda = 0$ line and the branches of the $\lambda = i\omega$ curve for $0 \le \kappa < -\beta$ (shown here, $\beta = -1$, $\kappa = 1/2$).* (a) $\tau_s^* < \tau_s < \tau_s^{(2)}$ *($\tau_s = 1.5$).* (b) $\tau_s > \tau_s^{(2)}$ *($\tau_s = 3$). The stability region is shaded, and the number of roots with positive real parts in other regions is as indicated. The lowest branch in* (a) *corresponds to τ_0^+.*

tion of γ_H and that the curve $\{(\gamma_H(\omega_2), \tau_j^+(\omega_2)) : \omega_{\min} \le \omega_2\}$ defines a curve $\{(\gamma_H, \tau_j^+(\gamma_H)) : \gamma_{\min} \le \gamma_H \le \kappa - \beta\}$ with τ_j^+ a continuous, decreasing function of γ_H. Since $\tau_j^-(\gamma_{\min}) = \tau_{j,\min}^- < \tau_{j,\min}^+ = \tau_j^+(\gamma_{\min})$, a straightforward argument shows that these curves intersect at one point $(\gamma_{\text{int}}, \tau_{\text{int}})$ in the region R_j^- and that $\tau_j^-(\gamma_H) < \tau_j^+(\gamma_H)$ for $\gamma_{\min} \le \gamma_H < \gamma_{\text{int}}$. Hence, in R_j^- the boundary of the stability region is given by the curves $\{(\gamma_H(\omega_1), \tau_j^-(\omega_1)) : \omega_{1,\text{int}} \le \omega_1 \le \omega_{\min}\}$ and $\{(\gamma_H(\omega_2), \tau_j^+(\omega_2)) : \omega_{\min} \le \omega_2 \le \omega_{2,\text{int}}\}$, where $\tau_j^-(\omega_{1,\text{int}}) = \tau_{\text{int}} = \tau_j^+(\omega_{2,\text{int}})$.

A similar result holds in the region

$$R_j^+ = \left\{(\gamma, \tau) : \gamma_{\min} \le \gamma \le \kappa - \beta, \quad \tau_{j,\min}^+ \le \tau \le \tau_{j+1,\min}^-\right\}.$$

For $\tau_s^{(1)} \le \tau_s \le \tau_s^*$, $\{(\gamma_H(\omega), \tau_1^-(\omega)) : \omega_{\min} \le \omega\}$, is the lowest branch of the $\lambda = i\omega$ curve. This establishes statement 2.

For $\tau_s > \tau_s^*$, $(\gamma_H(\omega), \tau_0^+(\omega))$, $0 \le \omega \le \omega_{\min}$, is the lowest branch of the $\lambda = i\omega$ curve. Noting that this branch intersects the γ-axis at $\gamma = \hat{\gamma} \ge \gamma_{\min}$ and never intersects the curve $(\gamma_H(\omega), \tau_1^-(\omega))$, $\omega_{\min} \le \omega$, establishes statement 3. □

Stability diagrams corresponding to this theorem are not shown, however, they appear qualitatively like those in Figures 3 and 4(a).

We now come to the final case $0 \le \kappa < -\beta$. In contrast to the previous cases, here it is possible for $\gamma_H(\omega)$ to be zero. The following lemma establishes when this occurs.

LEMMA 3. *Let κ and β be fixed. If $\kappa > |\beta|$, then $\gamma_H(\omega) \ne 0$ for any $\tau_s \ge 0$ and any $\omega \in (0, \infty)$. If $\kappa < |\beta|$, there exist a countable infinity of values of τ_s for which $\gamma_H(\omega) = 0$, for some $\omega \in (0, \infty)$.*

Proof. We begin by letting $\gamma = 0$ in (2.14) and (2.15) and assume that $\omega > 0$. This results in

$$\beta \cos(\omega\tau_s) = \kappa \quad \text{and} \quad \beta \sin(\omega\tau_s) = -\omega. \tag{2.23}$$

Clearly, these equations can be satisfied only if $\kappa < |\beta|$. In this case, squaring and adding (2.23) produce

$$\omega = \sqrt{\beta^2 - \kappa^2}. \tag{2.24}$$

Substituting this expression into the first equation of (2.23) and solving for τ_s, we obtain

$$\tau_s = \frac{1}{\sqrt{\beta^2 - \kappa^2}} \left\{ \operatorname{Arccos}\left(\frac{\kappa}{\beta}\right) + 2n\pi \right\}, \tag{2.25}$$

where Arccos is the principal branch of the inverse cosine function which has the range $[0, \pi]$, and we add multiples of 2π since for fixed β, $\sin(\omega\tau_s)$ never changes sign. □

Remark. We are particularly interested in the smallest positive value of τ_s for which the $\lambda = i\omega$ curve touches the τ-axis. We denote this value of τ_s by

$$\tau_s^{(2)} = \frac{1}{\sqrt{\beta^2 - \kappa^2}} \left\{ \operatorname{Arccos}\left(\frac{\kappa}{\beta}\right) \right\}, \qquad 0 \le \kappa < |\beta| \tag{2.26}$$

and refer to it as the *second transition point.*

We can now state our final stability theorem, which is illustrated in Figures 3 and 4.

THEOREM 9. *Let β, κ, and τ_s be fixed with $0 \le \kappa < -\beta$, and let $\tau_j^{\pm}$ be as defined in* (2.17). *Then we have the following.*

(1) *For $0 \le \tau_s < \tau_s^{(1)}$, the stability region is the vertical strip $0 < \gamma < \kappa - \beta$, $\tau \ge 0$.*

(2) *For $\tau_s^{(1)} \le \tau_s \le \tau_s^*$, the stability region is the set of the points (γ, τ), satisfying*
   (a) $0 < \gamma < \gamma_{\min}$, $\tau \ge 0$;
   (b) $\gamma_{\min} < \gamma < \kappa - \beta$,
      (i) $0 < \tau < \tau_1^- \le \tau_{1,\min}^-$;
      (ii) $\tau_{j,\min}^- \le \tau_j^- < \tau < \tau_j^+ \le \tau_{j,\min}^+$; *and*
      (iii) $\tau_{j,\min}^+ \le \tau_j^+ < \tau < \tau_{j+1}^- \le \tau_{j+1,\min}^-$
      for $j = 1, 2, \ldots$.

(3) *For $\tau_s^* < \tau_s < \tau_s^{(2)}$, the stability region is the set of points (γ, τ), satisfying*
   (a) $0 < \gamma < \gamma_{\min}$ *for all* $\tau \ge 0$;
   (b) $\gamma_{\min} < \gamma < \kappa - \beta$,
      (i) $\tau_{0,\min}^+ \le \tau_0^+ < \tau < \tau_1^- \le \tau_{1,\min}^-$;
      (ii) $\tau_{j,\min}^- \le \tau_j^- < \tau < \tau_j^+ \le \tau_{j,\min}^+$; *and*
      (iii) $\tau_{j,\min}^+ \le \tau_j^+ < \tau < \tau_{j+1}^- \le \tau_{j+1,\min}^-$
      where $\gamma_{\min} \to 0$ *as* $\tau_s \to \tau_s^{(2)}$
      for $j = 1, 2, \ldots$.

(4) *For $\tau_s \ge \tau_s^{(2)}$, there is no stability region.*

Proof. Statements (1), (2), and (3) are established as in Theorem 8. The fact that $\gamma_{\min} \to 0$ as $\tau_s \to \tau_s^{(2)}$ follows directly from Lemma 3. To establish statement (4), consider the line $\gamma = 0$. Along this line, $\Delta_+(\lambda) = \Delta_-(\lambda) = 0$ is the characteristic equation of the trivial solution of (1.2). It follows directly from studies of this equation [4, 17] that the characteristic equation (2.3) has two pairs of complex conjugate roots with nonnegative real parts. Appealing to Theorems 4, 5, and 6, and the ordering of the $\lambda = 0$ lines and the branches of the $\lambda = i\omega$ curve shows that this number can never decrease by more than 3 as γ increases. □

The case $a_{12}a_{21} < 0$. When we derived the characteristic equation corresponding to the linear DDE (2.1), we listed two different sets of characteristic equations. The one we have not yet discussed is related to the case $a_{12}a_{21} < 0$, i.e., the characteristic equation (2.4):

$$\Delta_+(\lambda)\Delta_-(\lambda) = \left(\lambda + \kappa - \beta e^{-\lambda\tau_s} + i\tilde{\gamma}e^{-\lambda\tau}\right)\left(\lambda + \kappa - \beta e^{-\lambda\tau_s} - i\tilde{\gamma}e^{-\lambda\tau}\right) = 0,$$

where $\tilde{\gamma} = \sqrt{-a_{12}a_{21}}$.

We shall not discuss this case in great depth; it suffices to say that Theorems 1, 2, and 3 can be slightly altered so that the conclusions are the same. Furthermore, $\tilde{\gamma}_H$ is defined exactly the same way as γ_H in (2.16), thus all theorems and lemmas relating to γ_H follow. Moreover, in this case $\tau_j^{\pm}$ are defined similarly to (2.17), the main difference lying in the argument of the Arctan function.

Notice that there is no $\lambda = 0$ line. Further, since Theorem 6 applies, the characteristic equation of the trivial fixed point gains a pair of complex conjugate eigenvalues when crossing the $\lambda = i\omega$ curve. Therefore, by Theorem 4, the boundary of the stability region must always be the $\lambda = i\omega$ curve. Hence, the stability region of the trivial fixed point is the region between the τ-axis and the $\lambda = i\omega$ curve, where the $\lambda = i\omega$ curve undergoes various qualitative changes depending on the values of the parameters.

In summary, for the case $a_{12}a_{21} < 0$ we know the following:

(1) For $\beta > 0$, $0 \le \kappa < \beta$, there is no stability region for all $\gamma \ge 0$, $\tau \ge 0$, and $\tau_s \ge 0$.
(2) For $\beta > 0$, $\kappa > \beta$, the stability region is defined by the region between the τ-axis and the $\lambda = i\omega$ curve, which undergoes one transition:
   (a) for $0 \le \tau_s < \tau_s^{(1)}$, the branches of the $\lambda = i\omega$ curve are nested;
   (b) for $\tau_s^{(1)} \le \tau_s$, the branches of the $\lambda = i\omega$ curve intersect.
(3) For $\beta < 0$, $0 \le \kappa < -\beta$, the stability region is defined by the region between the τ-axis and the $\lambda = i\omega$ curve, which undergoes two transitions:
   (a) for $0 \le \tau_s < \tau_s^{(1)}$, the branches of the $\lambda = i\omega$ curve are nested;
   (b) for $\tau_s^{(1)} \le \tau_s < \tau_s^{(2)}$, the branches of the $\lambda = i\omega$ curve intersect, and for $\tau_s > \tau_s^*$ an exceptional branch appears;
   (c) for $\tau_s \ge \tau_s^{(2)}$, the trivial fixed point has no region of stability.
(4) For $\beta < 0$, $\kappa > -\beta$, the $\lambda = i\omega$ curve undergoes one transition:
   (a) for $0 \le \tau_s < \tau_s^{(1)}$, the branches of the $\lambda = i\omega$ curve are nested;
   (b) for $\tau_s^{(1)} \le \tau_s$, the branches of the $\lambda = i\omega$ curve intersect, and once again, for $\tau_s > \tau_s^*$ an exceptional branch appears.

3. Bifurcations. In the previous section, we determined all points in parameter space where the characteristic equation (2.2) has roots with zero real parts, i.e., where the trivial fixed point of (1.2) has eigenvalues with zero real parts. Varying one or more parameters in the system (1.2) so as to pass through such a point may cause a *bifurcation*, i.e., a qualitative change in the type of solutions admitted by the DDE. Such points are important, particularly when they lie on the boundary of the stability region of the trivial fixed point, as they determine the overall behavior of the system.

The purpose of this section is to study the bifurcations which occur in (1.2) when a single parameter is varied. There are two such codimension one bifurcations: a steady state bifurcation, which can occur when the characteristic equation has a single zero eigenvalue, and a Hopf bifurcation, which can occur when the characteristic equation has a pair of pure imaginary eigenvalues. It should be clear from the results of the

previous section that both these bifurcations may occur when $a_{12}a_{21} > 0$, but only the Hopf bifurcation may occur when $a_{12}a_{21} < 0$. We will thus restrict our analysis to the former case, the analysis for the latter being similar. We perform numerical simulations for both cases.

For the case $a_{12}a_{21} > 0$, we shall choose the parameter γ as the one to vary to cause the bifurcations. While this seems natural based on the results of the previous section, and, in particular, Figures 2–4, this parameter does not appear explicitly in the original equation (1.2), thus some extra assumption is required. The discussion of the rest of this section will hence take place under the assumption that the parameters a_{12} and a_{21} may be written as continuously differentiable functions of the parameter γ via

$$a_{12} = f(\gamma), \qquad a_{21} = g(\gamma), \tag{3.1}$$

where $f(\gamma)g(\gamma) = \gamma^2$. Under these assumptions, the standard theory of bifurcations may be applied to (1.2) with γ as the distinguished parameter. Since we do not need to specify f and g explicitly, we shall be able to make quite general assertions about bifurcations in the system. Note that two particular cases included above are

$$f(\gamma) = \gamma = g(\gamma) \tag{3.2}$$

and

$$f(\gamma) = \text{constant}, \qquad g(\gamma) = \frac{\gamma^2}{\text{constant}}, \tag{3.3}$$

the latter being our choice for the numerical simulations.

For the simulations in the case $a_{12}a_{21} < 0$ we choose $\tilde{\gamma}$ as our distinguished parameter, with $a_{12} = \text{constant}$ and $a_{21} = -\tilde{\gamma}^2/\text{constant}$.

3.1. Steady state bifurcation. In this subsection we investigate the behavior of (1.2) in the neighborhood of a $\lambda = 0$ line. Recall from the previous section that the trivial fixed point exists for all parameter values and, for fixed β, κ, τ_s, and τ, satisfying $\tau > \tau^*$, as γ increases through a $\lambda = 0$ line, the characteristic equation (2.3) gains a positive real root (cf. Theorem 5). Thus, one might expect a steady state bifurcation to occur at these parameter values. In this subsection we will show that, indeed, the behavior associated with a pitchfork bifurcation occurs in the DDE (1.2) when γ passes through $\pm\gamma_0$.

The following two propositions establish the standard nondegeneracy conditions for a steady state bifurcation.

PROPOSITION 1. *The root $\lambda = 0$ of (2.3) is simple for almost all parameter values.*

Proof. From the characteristic equation (2.3), we find that the derivative of $\Delta_\pm(\lambda)$ with respect to λ is

$$\Delta'_\pm(\lambda) = 1 + \beta\tau_s e^{-\lambda\tau_s} \mp \tau\gamma e^{-\lambda\tau}.$$

Evaluating this at $\lambda = 0$ and recalling the location of these zero roots in parameter space ((2.12) and (2.13)) yields

$$\Delta'_\pm(\lambda)\big|_{\lambda=0} = 1 + \beta\tau_s + \tau(\kappa - \beta).$$

Thus, $\Delta'_\pm(\lambda)\big|_{\lambda=0} \neq 0$ so long as $\tau \neq \tau^*$, as defined in (2.19). Note that for $\beta > 0$ and $\kappa > \beta$, $\Delta'_\pm(\lambda)\big|_{\lambda=0} > 0$ for all $\tau \geq 0$ and $\tau_s \geq 0$.

Consider a point $(\pm\gamma_0, \tau)$ on a $\lambda = 0$ line. If $\tau \neq \tau^*$ and the point does not correspond to an intersection point with the $\lambda = i\omega$ curve, then there is only one root with $Re(\lambda) = 0$. □

PROPOSITION 2. *For fixed $\kappa \geq 0$, β, $\tau \geq 0$, and $\tau_s \geq 0$,*

$$\left.\frac{d\mathrm{Re}(\lambda)}{d\gamma}\right|_{\lambda=0,\gamma=\pm\gamma_0} \neq 0.$$

Proof. The result follows directly from the proof of Theorem 5. □

Propositions 1 and 2 indicate the possibility of a steady state bifurcation along $\gamma = \pm\gamma_0$. To determine the type of bifurcation which occurs, we investigate the existence of nontrivial fixed points of (1.2). Such fixed points must satisfy

$$x_1 = \frac{\beta}{\kappa}\tanh(x_1) + \frac{a_{12}}{\kappa}\tanh(x_2) \quad \text{and} \quad x_2 = \frac{a_{21}}{\kappa}\tanh(x_1) + \frac{\beta}{\kappa}\tanh(x_2)$$

for $\kappa > 0$. Isolation of x_1 and x_2 in turn yields the equivalent equations

$$x_2 = \frac{1}{a_{12}}\left[\beta x_1 + \frac{\gamma^2 - \beta^2}{\kappa}\tanh(x_1)\right] \equiv f(x_1) \tag{3.4}$$

and

$$x_1 = \frac{1}{a_{21}}\left[\beta x_2 + \frac{\gamma^2 - \beta^2}{\kappa}\tanh(x_2)\right] \equiv g(x_2), \tag{3.5}$$

where $\gamma = \sqrt{a_{12}a_{21}}$. Careful study of these equations leads to the following theorem.

THEOREM 10. *If $\gamma > |\kappa - \beta|$, then the DDE* (1.2) *has two nontrivial fixed points (x_1^*, x_2^*) and $(-x_1^*, -x_2^*)$.*

Proof. Consider the function

$$h(x_1) \equiv x_1 - g\left(f(x_1)\right). \tag{3.6}$$

It follows from (3.4)–(3.6) that

$$h(x_1) = \left(\tfrac{\gamma^2-\beta^2}{\kappa\gamma^2}\right)\Big[\kappa x_1 - \beta\tanh(x_1) - a_{12}\tanh\left\{\tfrac{1}{a_{12}}\left(\beta x_1 + \tfrac{\gamma^2-\beta^2}{\kappa}\tanh(x_1)\right)\right\}\Big]$$

for $\kappa > 0$. A straightforward calculation yields

$$\lim_{x_1\to 0^+}\frac{h(x_1)}{x_1} = \frac{\left(\gamma^2 - \beta^2\right)\left[(\kappa-\beta)^2 - \gamma^2\right]}{\kappa^2\gamma^2}$$

and

$$\lim_{x_1\to +\infty}\frac{h(x_1)}{x_1} = \frac{\gamma^2 - \beta^2}{\gamma^2}.$$

Thus, if $\gamma > |\kappa - \beta|$, then we have

$$\left(\lim_{x_1\to 0^+}\frac{h(x_1)}{x_1}\right)\left(\lim_{x_1\to +\infty}\frac{h(x_1)}{x_1}\right) < 0. \tag{3.7}$$

Since $h(x_1)$ is a continuous function, (3.7) implies that $h(x_1)$ has a positive root; call it x_1^*. Define $x_2^* = f(x_1^*)$, then (x_1^*, x_2^*) is a nontrivial solution of (3.4) and (3.5). Since $h(x_1)$ and $f(x_1)$ are odd functions, $(-x_1^*, -x_2^*)$ is also a solution of (3.4) and (3.5). □

THEOREM 11. *If $\beta < 0$, $\kappa \geq 0$, and $\gamma < \kappa - \beta$, then $(0,0)$ is the only fixed point of the DDE* (1.2).

Proof. Define $h(x_1)$ as in Theorem 10. Then

$$h'(x_1) \equiv 1 - g'\left(f(x_1)\right) f'(x_1),$$

and using (3.4) and (3.5), we find

$$\begin{aligned} h'(x_1) = \frac{\gamma^2 - \beta^2}{\kappa^2\gamma^2} \big\{ & \kappa^2 - \beta\kappa \left[\operatorname{sech}^2(x_1) + \operatorname{sech}^2(f(x_1))\right] \\ & -(\gamma^2 - \beta^2)\operatorname{sech}^2(x_1)\operatorname{sech}^2(f(x_1))\big\}. \end{aligned}$$

Note that $h(0) = 0$ and

$$h'(0) = \frac{\gamma^2 - \beta^2}{\kappa^2\gamma^2}\left[(\kappa - \beta)^2 - \gamma^2\right].$$

Clearly, if $\gamma^2 < \beta^2$, then $h'(x_1) < 0$ for all $x_1 \geq 0$. Since $h(0) = 0$, we have $h(x_1) \neq 0$ for $x_1 > 0$.

Consider now the case when $\gamma^2 > \beta^2$,

$$\begin{aligned} h'(x_1) &> \frac{\gamma^2 - \beta^2}{\kappa^2\gamma^2} \big\{ \kappa^2 \left[1 - \operatorname{sech}^2(f(x_1))\operatorname{sech}^2(x_1)\right] - \beta\kappa \left[\operatorname{sech}^2(x_1) + \operatorname{sech}^2(f(x_1))\right. \\ &\quad \left. -2\operatorname{sech}^2(f(x_1))\operatorname{sech}^2(x_1)\right]\big\}, \\ &> \frac{\gamma^2 - \beta^2}{\kappa^2\gamma^2} \left\{ \kappa^2 \left[1 - \operatorname{sech}^2(f(x_1))\operatorname{sech}^2(x_1)\right] - \beta\kappa \left[\operatorname{sech}(f(x_1)) - \operatorname{sech}(x_1)\right]^2 \right\}. \end{aligned}$$

Hence, $h'(x_1) > 0$ for $x_1 \geq 0$. Since $h(0) = 0$, we have $h(x_1) \neq 0$ for $x_1 > 0$.

Further, since $h(x_1)$ is odd, $h(x_1) \neq 0$ for $x_1 < 0$ in both cases. □

THEOREM 12. *If $\beta > 0$, $\kappa > 2\beta$, and $\gamma < \kappa - \beta$, then $(0,0)$ is the only fixed point of the nonlinear DDE* (1.2).

Proof. The proof is similar to that of Theorem 11, hence we will omit it. □

Remark. For a given set of parameter values, it is possible to study the existence of nontrivial fixed points of (1.2) by plotting (3.4) and (3.5) and looking for intersection points. Using this procedure we have never observed nontrivial fixed points for parameter values satisfying $0 < \gamma < \kappa - \beta$ and have observed up to four nontrivial fixed points for parameter values satisfying $0 < \gamma < \beta - \kappa$.

Based on these results, we make the following conjectures.

CONJECTURE 1. *For fixed $\beta > 0$, $\tau \geq 0$, $\tau_s \geq 0$, $\kappa \geq 0$, and any a_{12}, a_{21} satisfying* (3.1), *the trivial fixed point of the DDE* (1.2) *undergoes a pitchfork bifurcation at $\gamma = |\kappa - \beta|$. If $\kappa > \beta$, this bifurcation is supercritical, and for $0 < \gamma < \kappa - \beta$, the trivial fixed point is stable and attracts all solutions. If $\beta > \kappa$, the bifurcation is subcritical.*

CONJECTURE 2. *Let $\beta < 0$, $\tau \geq 0$, $\tau_s \geq 0$, $\kappa \geq 0$, and a_{12}, a_{21} satisfying* (3.1) *be fixed. Suppose that $\tau \neq \tau^*$ and that $(\kappa - \beta, \tau)$ does not correspond to an intersection point of the $\lambda = i\omega$ curve and the $\lambda = 0$ line. Then the trivial fixed point of the*

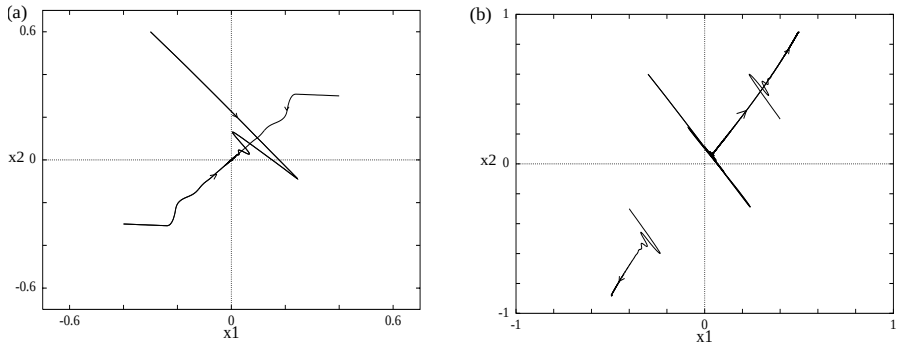

FIG. 5. *Numerical simulations of* (1.2) *for the three initial conditions* (3.8), (3.9), *and* (3.10). *Parameter values are* $\beta = -1$, $\kappa = 1/2$, $\tau_s = 0.01$, $\tau_1 = \tau_2 = 1$, $a_{12} = 1$. (a) $a_{21} = 1.2$, *corresponding to* $\gamma < \kappa - \beta$. *All solutions are asymptotic to the stable fixed point at* $(0, 0)$. (b) $a_{21} = 2.5$, *corresponding to* $\gamma > \kappa - \beta$. *Solutions tend to either the fixed point at* $(x_1^*, x_2^*) = (0.496, 0.881)$ *or the fixed point at* $(-x_1^*, -x_2^*) = (-0.496, -0.881)$. *Solutions are shown in the* x_1, x_2 *plane.*

nonlinear DDE (1.2) *undergoes a supercritical pitchfork bifurcation at* $\gamma = \kappa - \beta$. *If* τ_s *satisfies* $0 < \tau_s < \tau_s^{(1)}$, *then the trivial fixed point is stable for* $0 < \gamma < \kappa - \beta$ *and attracts all solutions.*

To determine with certainty the type of steady state bifurcations which occur in this system would require analyzing the stability of the fixed points (x_1^*, x_2^*) and $(-x_1^*, -x_2^*)$. To do this, we would need to linearize the DDE (1.2) about these fixed points, produce a new characteristic equation, and analyze its roots. This is a large task, certainly beyond the scope of this paper. Instead, we provide numerical evidence to support our conjectures.

3.1.1. Numerical simulations near the $\boldsymbol{\lambda = 0}$ line. In this subsection we supplement our steady state bifurcation argument with numerical simulations of the evolution of solutions of the original nonlinear DDE (1.2). All simulations shown here and in the following sections were performed with the package XPP by Ermentrout [8] using one of the following initial conditions:

$$x_1(t) = 0.4 \qquad x_2(t) = 0.3 \qquad -h \le t \le 0, \tag{3.8}$$

$$x_1(t) = -0.4 \qquad x_2(t) = -0.3 \qquad -h \le t \le 0, \tag{3.9}$$

$$x_1(t) = -0.3 \qquad x_2(t) = 0.6 \qquad -h \le t \le 0, \tag{3.10}$$

$h = \max\{\tau_s, \tau\}$, unless otherwise indicated. We have, however, performed experiments using a variety of initial conditions.

Experiment 1: $0 < \beta < \kappa$.

We observe that solutions with parameters satisfying $\gamma < \kappa - \beta$ tend to the origin. Furthermore, we observe that solutions having parameter values satisfying $\gamma > \kappa - \beta$ tend to the nontrivial fixed points. These simulations support Conjecture 1, i.e., that there is a supercritical pitchfork bifurcation at $\gamma = \kappa - \beta$.

Experiment 2: $0 < \kappa < \beta$.

We observe that solutions always converge to a nontrivial fixed point, i.e., the behavior of the system is unaffected by the bifurcation at $\gamma = \beta - \kappa$. This is expected as this bifurcation does not form part of the boundary of the stability region (c.f. Theorem 3).

Experiment 3: $\beta < 0$, $0 < \tau_s < \tau_s^{(1)}$.

We find that solutions with parameter values satisfying $\gamma < \kappa - \beta$ tend to the stable fixed point at $(0, 0)$, as predicted by our stability analysis. An example is shown in Figure 5(a), where we chose $\beta = -1$, $\kappa = 1/2$, $\tau_s = 0.01$, $a_{12} = 1$, $a_{21} = 1.2$, $\tau = 1$ (corresponding to the"x" in Figure 3(a)), and used (3.8), (3.9), and (3.10). We further find that solutions with parameter values satisfying $\gamma > \kappa - \beta$ tend to a nontrivial fixed point. An example is shown in Figure 5(b), where we let $\beta = -1$, $\kappa = 1/2$, $\tau_s = 0.01$, $a_{12} = 1$, $a_{21} = 2.5$, $\tau = 1$ (corresponding to the "+" in Figure 3(a)), and used (3.8) and (3.10). In this case, solving (3.4) and (3.5) numerically in Maple shows that that the fixed point, rounded to three decimal places, is $(x_1^*, x_2^*) = (0.496, 0.881)$, which agrees with Figure 5(b). Using the same parameter values, but initial conditions (3.9) yields a solution which tend toward the stable fixed point $(-x_1^*, -x_2^*) = (-0.496, -0.881)$. This supports Conjecture 2, namely, that a supercritical pitchfork bifurcation occurs.

Experiments for the case $\beta < 0$, $\tau_s > \tau_s^{(1)}$ will be discussed in section 3.2.

3.2. Hopf bifurcation. In this subsection we consider the behavior of the nonlinear DDE (1.2) in the neighborhood of the $\lambda = i\omega$ curve. Section 2 showed that the characteristic equation associated with the trivial fixed point has a pair of complex conjugate imaginary roots along this curve, thus we might expect (1.2) to exhibit a Hopf bifurcation along this curve. In the following we prove, via Propositions 3 and 4 and Theorem 13, that a Hopf bifurcation does occur along this curve when $a_{12}a_{21} > 0$. The argument in the case $a_{12}a_{21} < 0$ is similar.

We begin by establishing the usual nondegeneracy conditions on the roots of the characteristic equation.

PROPOSITION 3. *Consider a purely imaginary root $\lambda_c = i\omega_c$ of the characteristic equation* (2.3)*. Then λ_c is simple and all roots λ other than λ_c and $\bar{\lambda}_c$ satisfy $\lambda \neq m\lambda_c$ for any integer m, for almost all choices of the parameters.*

Proof. To show that $\lambda_c = i\omega_c$ is simple, we need to show that $\Delta'_{\pm}(\lambda_c) \neq 0$, where

$$\Delta'_{\pm}(\lambda) = 1 + \beta\tau_s e^{-\lambda\tau_s} \mp \tau\gamma e^{-\lambda\tau} \tag{3.11}$$

by (2.3). Suppose that $\Delta'_{\pm}(\lambda_c) = 0$. Substituting $\lambda_c = i\omega_c$, separating (3.11) into real and imaginary parts, we get

$$\beta\tau_s \cos(\omega_c\tau_s) + 1 = \pm\tau\gamma_H \cos(\omega_c\tau) \tag{3.12}$$

and

$$\beta\tau_s \sin(\omega_c\tau_s) = \pm\tau\gamma_H \sin(\omega_c\tau). \tag{3.13}$$

Consider the ratio of (3.13) and (3.12)

$$\tan(\omega_c\tau) = \frac{\beta\tau_s \sin(\omega_c\tau_s)}{\beta\tau_s \cos(\omega_c\tau_s) + 1}. \tag{3.14}$$

Furthermore, ω_c must satisfy

$$\tan(\omega_c\tau) = \frac{\beta\sin(\omega_c\tau_s)+\omega_c}{\beta\cos(\omega_c\tau_s)-\kappa}, \tag{3.15}$$

the ratio of (2.14) and (2.15), which are the real and imaginary parts of (2.3) when $\gamma=\gamma_H$ and $\lambda_c = i\omega_c$. Equating (3.14) and (3.15), we get

$$\frac{\beta\sin(\omega_c\tau_s)+\omega_c}{\beta\cos(\omega_c\tau_s)-\kappa} = \frac{\beta\tau_s\sin(\omega_c\tau_s)}{\beta\tau_s\cos(\omega_c\tau_s)+1}.$$

Cross-multiplying, we obtain

$$\omega_c + \beta\omega_c\tau_s\cos(\omega_c\tau_s) + \beta\sin(\omega_c\tau_s) = -\beta\kappa\tau_s\sin(\omega_c\tau_s).$$

Define $\Upsilon(\omega_c) = \omega_c + \beta\omega_c\tau_s\cos(\omega_c\tau_s) + \beta(1+\kappa\tau_s)\sin(\omega_c\tau_s)$. We note that $\Upsilon(\omega_c)$ is identical to the numerator of (2.21). Hence, by Lemma 2, $\Upsilon(\omega_c)>0$ for all $\tau_s<\tau_s^{(1)}$. Moreover, zeros of $\Upsilon(\omega_c)$ occur when $\frac{d\gamma_H}{d\omega}|_{\omega=\omega_c}=0$. Hence, when $\Delta_\pm'(\lambda)=0$, then these values of ω_c correspond to points satisfying $\frac{d\gamma_H}{d\omega}|_{\omega=\omega_c}=0$. Therefore, excluding the values of ω_c satisfying $\frac{d\gamma_H}{d\omega}|_{\omega=\omega_c}=0$, $\lambda_c=i\omega_c$ is a simple root of (2.3).

Further, if the point (γ_H,τ) in the $\gamma\tau$-plane does not correspond to an intersection point of two branches of the $\lambda=i\omega$ curve nor an intersection point of the $\lambda=i\omega$ curve and a $\lambda=0$ line, then there is only one pair of eigenvalues with $\mathrm{Re}(\lambda)=0$ at this point. Thus, for any other root $\lambda\neq\pm mi\omega_c$, for any $m\in\mathbb{Z}$. □

PROPOSITION 4. *$\frac{d\mathrm{Re}\lambda}{d\gamma}|_{\lambda_c=i\omega_c}=0$ if and only if ω_c satisfies $\frac{d\tau_j^\pm}{d\omega}|_{\omega=\omega_c}=0$, $\gamma_H(\omega_c)\neq 0$ and $\frac{d\gamma}{d\omega}|_{\omega\neq\omega_c}\neq 0$.*

Proof. The result follows from the proof of Theorem 6. □

Remark. Since the zeros of $\frac{d\mathrm{Re}\lambda}{d\gamma}$ correspond to points, where $\frac{d\tau}{d\omega}=0|_{\omega=\omega_c}$ and $\frac{d\gamma}{d\omega}|_{\omega=\omega_c}\neq 0$, then the zeros of $\frac{d\mathrm{Re}\lambda}{d\gamma}$ occur where the $\lambda=i\omega$ curve has a horizontal tangent line.

THEOREM 13. *Suppose that β, $\kappa\geq 0$, $\tau_s\geq 0$, and $\tau=\tau_c\geq 0$ are fixed and that (γ_c,τ_c) is a point on the $\lambda=i\omega$ curve that does not correspond to an intersection point of the branches of the $\lambda=i\omega$ curve or an intersection point of the $\lambda=i\omega$ curve and a $\lambda=0$ line. Denote by $i\omega_c$ the purely imaginary root of* (2.3) *which is such that $\gamma_c=\gamma_H(\omega_c)$, and $\tau_c=\tau_j^\pm(\omega_c)$ for some j, where $\gamma_H(\omega)$ and $\tau_j^\pm(\omega)$ are defined by* (2.16) *and* (2.17). *Assume that ω_c is neither a zero of $\frac{d\gamma_H}{d\omega}$ nor of $\frac{d\tau_j^\pm}{d\omega}$. Then the nonlinear DDE* (1.2) *undergoes a Hopf bifurcation at $\gamma=\gamma_c$.*

Proof. We begin by noting that (1.2) may be written in the standard form

$$\dot{x}(t) = F(\gamma, x_t), \tag{3.16}$$

where $x_t\in\mathcal{C}$, $F:\mathbb{R}\times\mathcal{C}$, $\mathcal{C}=C([-h,0],\mathbb{R}^2)$, when we take

$$F(\gamma,x_t) = \begin{pmatrix} -\kappa x_{1t}(0)+\beta\tanh\left(x_{1t}(-\tau_s)\right)+a_{12}\tanh(x_{2t}(-\tau)) \\ -\kappa x_{2t}(0)+\beta\tanh\left(x_{2t}(-\tau_s)\right)+a_{21}\tanh(x_{1t}(-\tau)) \end{pmatrix}$$

and let a_{12}, a_{21} be given by (3.1). It is then straightforward to show that F has continuous first and second derivatives with respect to both γ and ϕ (see [25] for details).

Propositions 3 and 4 imply that (3.16) obeys the conditions of the Hopf bifurcation theorem [14, p. 333] and the result follows. □

It is well known [14] that the behavior of a DDE such as (1.2) in the neighborhood of a point of the Hopf bifurcation is determined by the following system of ODEs (in polar coordinates)

$$\dot{r} = \mu r + a r^3,$$
$$\dot{\theta} = \omega.$$

In particular, if $a > 0$, the Hopf bifurcation is supercritical and if $a < 0$, it is subcritical. Using the centre manifold and normal form techniques, this coefficient may be related to parameters in the DDE (see [2], [5], [27] for details of this computation).

We have used a Maple program [5] to determine the coefficient a for the first four branches of the $\lambda = i\omega$ curve shown in Figures 3(b) and 4(a) for the parameterization given in (3.1)–(3.3). We see the following behavior. In some cases, the bifurcation is supercritical along the whole branch. In other cases, the bifurcation is supercritical for large values of τ, but becomes subcritical as τ decreases. In a few cases, we observed several switches between supercritical and subcritical bifurcations along a single branch. The point or points where the criticality changes (which corresponds to a well studied [10] degenerate Hopf bifurcation) usually occur to the right of the $\lambda = 0$ line and thus will not have a large effect on the observable behavior of the system. Of particular note is the fact that even when β, κ, τ_s, τ, and γ are fixed, changing the parameterization of a_{12} and a_{21} (i.e., changing f and g in (3.1)) can change the criticality of the bifurcation. This is because the coefficient a depends on both a_{12} and a_{21} independently and not just their product, γ^2.

3.2.1. Numerical simulations near the $\lambda = i\omega$ curve.

Experiment 1: $0 < \beta < \kappa$, $a_{12}a_{21} > 0$ or $\beta < 0$, $0 < \tau_s < \tau_s^{(1)}$, $a_{12}a_{21} > 0$.
We observe that solutions always converge to a nontrivial fixed point. This is expected since, in these cases, the Hopf bifurcation curves occur to the right of the $\lambda = 0$ line, where the trivial fixed point is already unstable.

Experiment 2: $\beta < 0$, $\tau_s^{(1)} < \tau_s < \tau_s^{(2)}$, $a_{12}a_{21} > 0$ or $0 < \tau_s < \tau_s^{(2)}$, $a_{12}a_{21} < 0$.
In this case, the branches of the $\lambda = i\omega$ curve are, qualitatively, as shown in Figures 3(b) and 4(a). Choosing parameter values to the left of the $\lambda = i\omega$ curve, we observe solutions that tend to the origin, while parameter values in the region marked 2 (in Figures 3(b) and 4(a)) produce solutions which tend to a stable periodic orbit.
This experiment provides evidence that a supercritical Hopf bifurcation of the trivial fixed point occurs for parameter values crossing from the stability region to the region marked 2 in Figures 3(b) and 4(a).

Experiment 3: $\beta < 0$, $\tau_s > \tau_s^{(2)}$.
We observe that solutions always converge to a periodic orbit or to a nontrivial fixed point. This is expected since this bifurcation curve does not form part of the boundary of the stability region (cf. Theorem 9).

4. Interaction of bifurcations. In the previous sections, we described the location of various bifurcations in the $\gamma\tau$ parameter space. In particular, we provided analytical and numerical evidence that pitchfork bifurcations occur along the $\lambda = 0$ lines (2.12) and (2.13) and that Hopf bifurcations occur along the various branches of the $\lambda = i\omega$ curve, (2.16) and (2.17) in the case $a_{12}a_{21} > 0$. It is evident from the results of section 2, as shown for example in Figure 4, that intersections of these

various lines and curves may occur. Such intersection points correspond to bifurcation interaction points, also known as codimension two bifurcation points. In this section, we describe the bifurcation interactions which can occur in the DDE (1.2) and show how these interactions influence the behavior observed in the system.

There are three main ways in which the bifurcation curves can intersect leading to the following three types of bifurcation interaction points.

(1) *Hopf-Hopf interaction:* This occurs where two branches of the $\lambda = i\omega$ curve intersect transversally. It corresponds to a point where the characteristic equation (2.2) has two pairs of pure imaginary roots.
(2) *Hopf-pitchfork interaction:* This occurs where a branch of the $\lambda = i\omega$ curve intersects a $\lambda = 0$ line transversally. It corresponds to a point where the characteristic equation (2.2) has a pair of pure imaginary roots and a zero root.
(3) *Takens–Bogdanov interaction:* This occurs where the exceptional branch of the $\lambda = i\omega$ curve terminates on a $\lambda = 0$ line. It corresponds to a point where the characteristic equation (2.2) has a double zero root.

The various lemmas and theorems of section 2 indicate where in parameter space these interactions may occur, as summarized below.

- $a_{12}a_{21} > 0,\ \beta > 0$: Interactions occur outside the region of stability of the trivial fixed point and thus do not affect the observable dynamics of the system.
- $a_{12}a_{21} > 0,\ \beta < 0$: Interactions 1 and 2 occur if and only if $\tau_s \geq \tau_s^{(1)}$. Interaction 3 occurs if and only if $\tau_s > \tau_s^*$.
- $a_{12}a_{21} < 0$: Interaction 1 occurs if and only if $\tau_s \geq \tau_s^{(1)}$. Interactions 2 and 3 do not occur.

Note that for each value of τ_s where these interactions can occur, there are a countable infinity of interaction points of types 1 and 2 but only one of type 3.

Using a center manifold reduction [14], it can be shown that the dynamics of systems of DDEs, such as (1.2), in the neighborhood of a bifurcation interaction point are determined by a system of ODEs, whose dimension corresponds to the number of roots of the characteristic equation with zero real parts at the interaction point. Using normal form analysis, the behavior of the system of ODEs corresponding to each of the interaction types described above has been studied in depth [13, Chapter 7], [18, Chapter 8]. The details of these computations and of a Maple program designed to perform them symbolically are described in [5]. In the rest of this section, we use the results of this program to predict the behavior of system (1.2) in the neighborhood of interaction points of the three types described above, and compare the predictions with numerical simulations of the full system of DDEs.

4.1. Hopf-Hopf interaction. Recall from section 3 that the Hopf bifurcations which occur in system (1.2) on the boundary of the region of stability of the fixed point are, for the most part, supercritical. As shown in Guckenheimer and Holmes [13, section 7.5], the interaction of two such supercritical Hopf bifurcations results in a secondary Hopf bifurcation leading to the creation of a 2-torus. We have applied the Maple program described above to several Hopf-Hopf interaction points on the boundary of the stability region in Figures 3(b) and 4(a). In all cases, we find that the parameter values are such that the torus is unstable and coexists with two stable limit cycles (one resulting from each of the primary Hopf bifurcations). This is confirmed by numerical simulations of (1.2) with parameter values near any one of these interaction points. An example is shown in Figure 6, where the parameter values correspond to

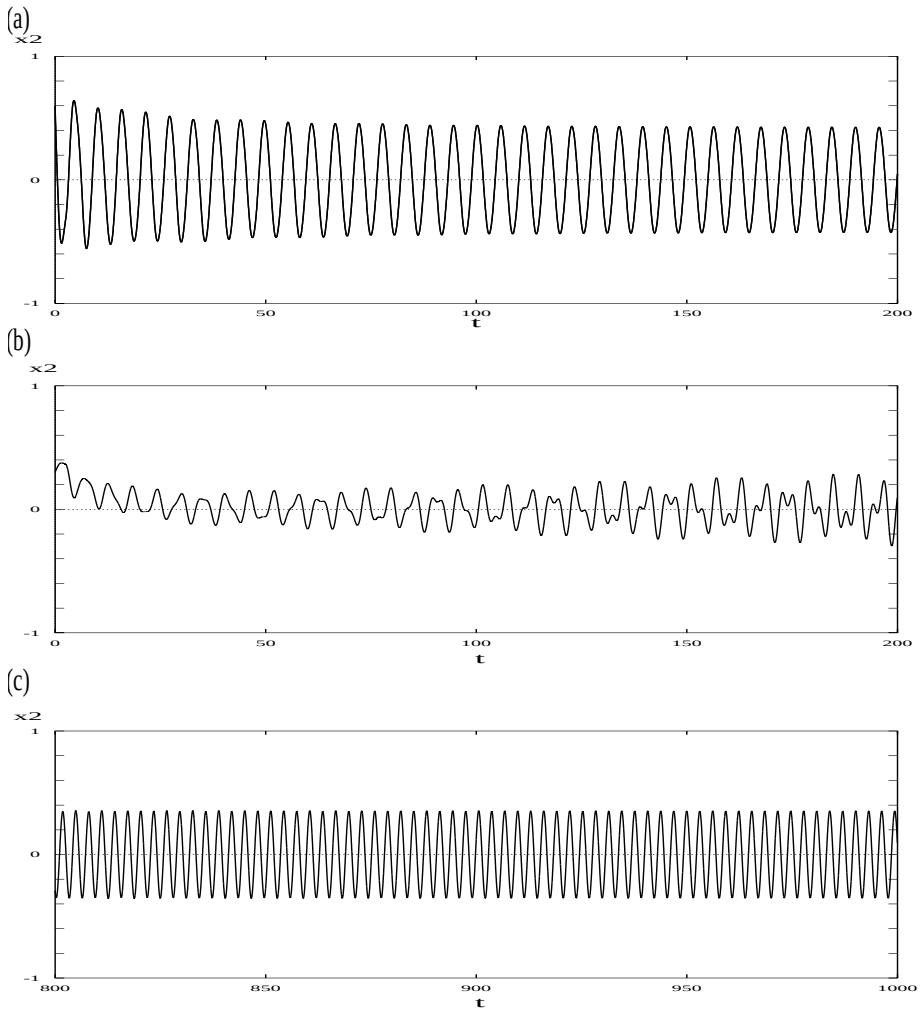

FIG. 6. *Numerical simulations of* (1.2) *with* $\beta = -1$, $\kappa = 1/2$, $\tau_s = 0.8$, $\tau_1 = \tau_2 = 2.5$, $a_{12} = 1$, $a_{21} = 1.39$. (a) *Initial condition* (3.10). (b) *Transient behavior, initial condition* (3.8). (c) *Longterm behavior, initial condition* (3.8). *Solutions are shown as* x_2 *time histories.*

the intersection point of the lower two branches of the $\lambda = i\omega$ curve in Figure 3(b). When the initial condition (3.10) is used, the system tends to one limit cycle (Figure 6 (a)). When the initial condition (3.8) is used, however, the system initially behaves quasiperiodically (Figure 6 (b)) and ultimately settles on a second limit cycle (Figure 6 (c)).

4.2. Hopf-pitchfork interaction. This interaction is also discussed in [13, section 7.5] where it is shown that when both bifurcations are supercritical (as is our situation, see section 3), a secondary bifurcation leading to the creation of two limit cycles not surrounding the origin results. Again, applying the Maple program to several interaction points yields the same qualitative results: the parameters are such that these new limit cycles are unstable and coexist with two stable, nontrivial fixed points and a stable limit cycle surrounding the origin. These results are confirmed by

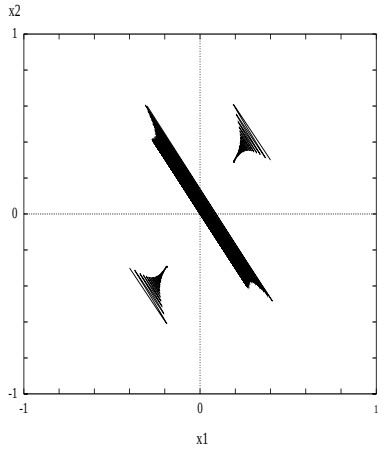

FIG. 7. *Numerical simulation of* (1.2) *with* $\beta = -1$, $\kappa = 1/2$, $\tau_s = 0.8$, $\tau_1 = \tau_2 = 0.7$, $a_{12} = 1$, $a_{21} = 2.28$. *Three solutions, corresponding to initial conditions* (3.8), (3.9), *and* (3.10), *are shown in the* x_1, x_2 *plane.*

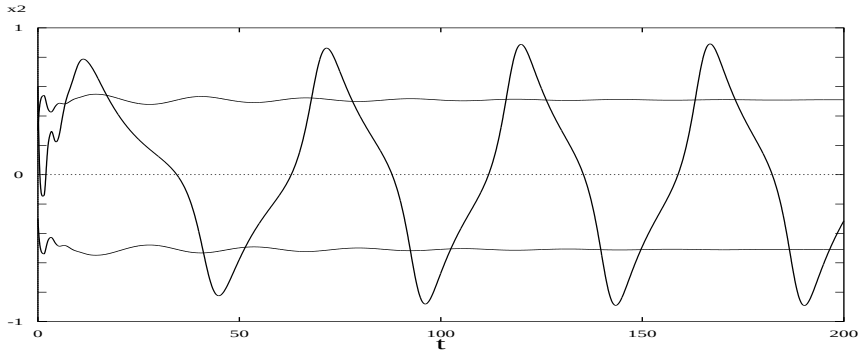

FIG. 8. *Numerical simulation of* (1.2) *with* $\beta = -1$, $\kappa = 1/2$, $\tau_s = 1.5$, $\tau_1 = \tau_2 = 0.2$, $a_{12} = 1$, $a_{21} = 2.34$. *Three solutions, corresponding to initial conditions* (3.8), (3.9), *and* (3.10), *are shown as superimposed* x_2 *time histories.*

numerical simulations of (1.2), an example of which is shown in Figure 7.

4.3. Takens–Bogdanov interaction. In [13, section 7.3], it is shown that when the Takens–Bogdanov interaction involves a supercritical Hopf and a supercritical pitchfork bifurcation, one should expect to find a region of parameter space in which the nontrivial fixed points are stable and coexist with a large amplitude, stable limit cycle which surrounds them. We observe this behavior in our numerical simulations of (1.2), an example of which is shown in Figure 8.

5. Discussion. In this paper, we have given a detailed analysis of the mathematical properties of the system of DDEs (1.2), emphasizing the implications of having time delays. In this section, we will review some of the important mathematical results obtained and discuss their meaning in the context of neural networks.

Perhaps the most interesting aspect of the analysis in section 2, of the stability of the trivial solution, is the fact that all the results depend on the connection parameters only through the product of the strengths, $a_{12}a_{21}$, and the sum of the delays, $\tau_1 + \tau_2$. In particular this means that the stability results for a system with two inhibitory

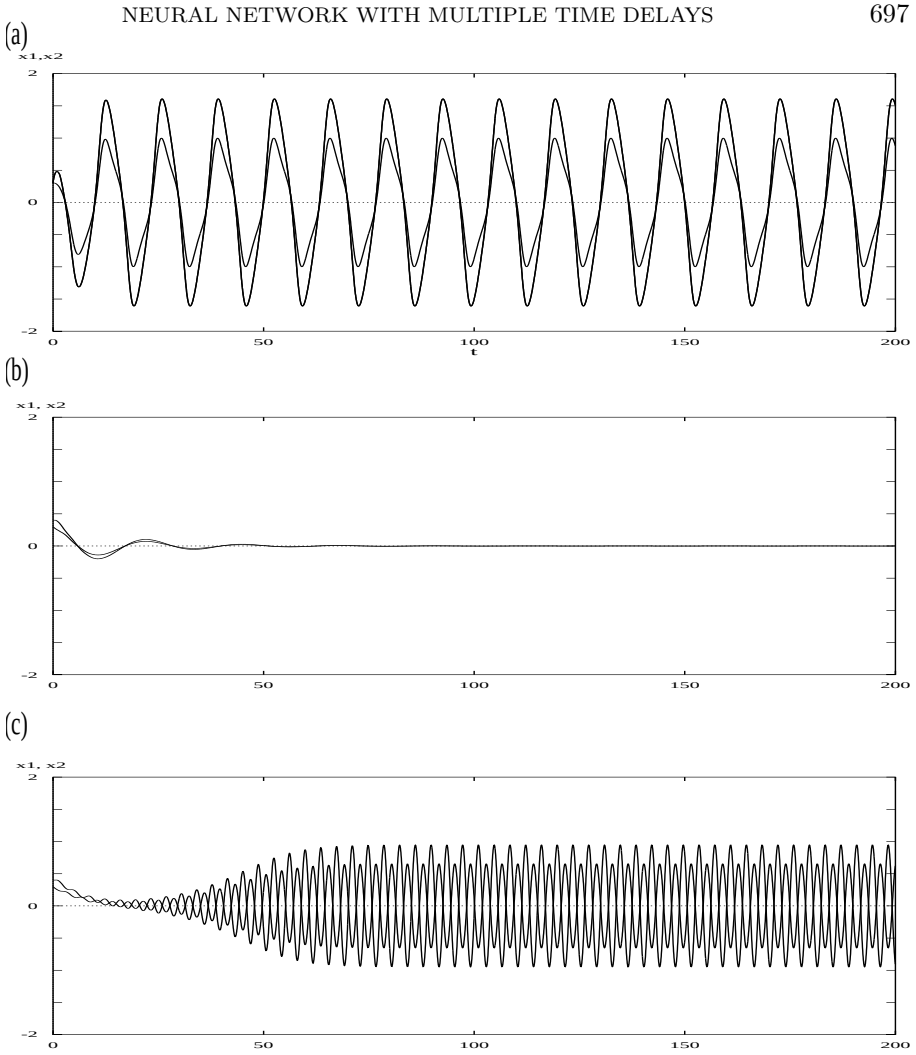

FIG. 9. *Numerical simulation of* (1.2) *with parameter values* $\beta = -1$, $\kappa = 1/2$, $\tau_s = 1.5$, $a_{12} = 1$ *and* $a_{21} = 2$ *(corresponding to Figure* 4(a)) *and initial condition* (3.8). (a) *In phase oscillation of two neurons occur when the connection time delays,* τ_1 *and* τ_2*, are both zero.* (b) *"Death" of the oscillation occurs when the connection time delays are increased to* $\tau_1 = \tau_2 = 0.4$. (c) *Out of phase oscillation occurs when the connection delays are large enough (*$\tau_1 = \tau_2 = 1$*). Solutions are shown as* x_1 *and* x_2 *time histories, superimposed.*

connections are identical to those for as a system with two excitatory connections of the same magnitude. Similar results have been observed in ring neural networks [1, 4] with an even number of elements.

The effect of the feedback on the stability results comes down to a certain critical value, $\tau_s^{(1)}$, of the delay which is determined by the circuit parameter κ and the strength of the feedback β. If the feedback delay, τ_s, is smaller than this value, the system behaves in a similar manner to systems without feedback such as those studied in [1, 12]. That is, its behavior is characterized by large regions of connection-delay independent stability and regions of global stability (see [25] for details) of the trivial fixed point, and the only other solutions possible are simple periodic or nontrivial fixed

points. If the feedback delay is larger than this value, more complicated behavior may arise, as discussed below.

In section 3, we showed that increasing the magnitude of either of the connection strengths, a_{ij}, can cause the trivial fixed point to lose stability via a pitchfork bifurcation giving rise to stable nontrivial fixed points or via a Hopf bifurcation giving rise to a stable periodic solution. These latter solutions dominate the parameter space, existing (and most often being the attractor of the system) in all regions in Figures 2–4 which are neither in the stability region nor in a region marked with "1". The presence of these solutions in our model is primarily due to the presence of time delays, as similar models without delays can be shown to be globally stable [6]. It should be clear from Figures 2–4 that Hopf bifurcations may also be caused by changing either of the connection delays, τ_1, τ_2. Thus, the common belief that delays can destabilize a stable fixed point giving rise to a periodic solution is true in this system. However, contrary to this view, increasing the connection delays in our system can also stabilize the trivial fixed point (this can be seen in Figures 3(b) and 4(a)). This phenomenon is quite common in systems with multiple time delays [2] and higher order systems with a single time delay [3, 7].

In section 4, we showed that when the feedback delay is larger than the critical value $\tau_s^{(1)}$, interactions of the various bifurcations may occur, giving rise to multistability. Interaction of a pitchfork bifurcation with a Hopf bifurcation gives rise to multistability between a pair of nontrivial fixed points and a periodic solution. When the parameters are in this state, small perturbations to the variables can cause the system to initiate or terminate oscillations. This type of *oscillator death* is observed in many systems including in a certain experimental culture of neurons [16]. Interactions of two Hopf bifurcations give rise to bistability between two limit cycles of different frequencies. This is interesting as it is generally believed that periodic firing is one mechanism for transmitting information in the nervous system [9], with the frequencies of the oscillations being the "message" transmitted. Thus, bistability between limit cycles provides a mechanism for the system to convey two different "messages" in response to different stimuli, for the same parameter values.

Finally, we present some other interesting behavior seen in our system. As noted in the introduction and seen in Figure 4, under certain conditions on the feedback parameters, the system will oscillate even when the connection delays or strengths are zero. In this parameter region, the neurons behave like a system of coupled oscillators and exhibit some of the associated behavior. For example, it is possible to destroy the oscillations in the system by increasing the connection time delay, as pictured in Figures 9 (a) and (b). This phenomenon of *oscillator death* due to time delays has recently been noted in a quite different system of coupled oscillators [22], and may, in fact, be quite common in oscillators with time delayed coupling. Further, as discussed in Schuster [24], delayed coupling may introduce a phase shift in the oscillations. This effect is quite interesting for it can give rise to solutions which are counterintuitive. As an example consider two neurons coupled together with excitatory connections. One might expect that they should oscillate in phase, which is what we observe in our system when the connection delay is zero (Figure 9(a)). However, if the connection delay is large enough we observe that they oscillate 180° out of phase (Figure 9(c)). The opposite effect is observed when the connections are inhibitory (see [25] for an example). This is important from an experimental viewpoint as it means that two neurons observed to be oscillating synchronously may have excitatory coupling with small time delays, or inhibitory coupling with large time delays.

Acknowledgments. We wish to thank John Wainwright for many useful discussions and the reviewers for their comments, which led to a clearer presentation of our results.

REFERENCES

[1] P. Baldi and A. Atiya, *How delays affect neural dynamics and learning*, IEEE Trans. Neural Networks, 5 (1994), pp. 612–621.

[2] J. Bélair and S. A. Campbell, *Stability and bifurcations of equilibria in a multiple delayed differential equation*, SIAM J. Appl. Math., 54 (1994), pp. 1402–1423.

[3] J. Bélair, S. A. Campbell, and P. van den Driessche, *Frustration, stability, and delay-induced oscillations in a neural network model*, SIAM J. Appl. Math., 56 (1996), pp. 245–255.

[4] S. A. Campbell, *Stability and bifurcation of a simple neural network with multiple time delays*, in Differential Equations with Application to Biology, S. Ruan, G. S. K. Wolkowicz, and J. Wu, eds., Fields Institute Commun. 21, AMS, Providence, RI, 1998, pp. 65–79.

[5] S. A. Campbell and J. Bélair, *Analytical and symbolically-assisted investigation of Hopf bifurcation in delay-differential equations*, Canad. Appl. Math. Quart., 3 (1995), pp. 137–154.

[6] M. A. Cohen and S. Grossberg, *Absolute stability of global pattern formation and parallel memory storage by competitive neural networks*, IEEE Trans. Systems, Man, and Cybernetics, 13 (1983), pp. 815–826.

[7] K. Cooke and Z. Grossman, *Discrete delay, distributed delay and stability switches*, J. Math. Anal. Appl., 86 (1982), pp. 592–627.

[8] B. Ermentrout, *XPPAUT*3.0—*The Differential Equations Tool*, University of Pittsburgh, Pittsburgh, 1997.

[9] D. Ferster and N. Spruston, *Cracking the neuronal code*, Science, 270 (1995), pp. 756–757.

[10] M. Golubitsky and W.F. Langford, *Classification and unfoldings of degenerate Hopf bifurcations*, J. Differential Equations, 41 (1981), pp. 375–415.

[11] K. Gopalsamy and X. He, *Stability in asymmetric Hopfield nets with transmission delays*, Phys. D, 76 (1994), pp. 344–358.

[12] K. Gopalsamy and I. Leung, *Delay induced periodicity in a neural netlet of excitation and inhibition*, Phys. D, 89 (1996), pp. 395–426.

[13] J. Guckenheimer and P. Holmes, *Nonlinear Oscillations, Dynamical Systems, and Bifurcations Vector Fields*, Springer-Verlag, New York, 1983.

[14] J. Hale and S. Lunel, *Introduction to Functional Differential Equations*, Springer-Verlag, New York, 1993.

[15] J. J. Hopfield, *Neurons with graded response have collective computational properties like two-state neurons*, Proc. Natl. Acad. Sci. U.S.A., 81 (1984), pp. 3088–3092.

[16] D. Kleinfeld, F. Raccuia-Behling, and H. Chiel, *Circuits constructed from identified aplysia neurons neurons exhibit multiple patterns of persistent activity*, Biophys. J., 57 (1990), pp. 697–715.

[17] V. Kolmanovskii and V. Nosov, *Stability of Functional Differential Equations*, Academic Press, Toronto, 1986.

[18] Y. Kuznetsov, *Elements of Applied Bifurcation Theory*, Appl. Math. Sci. 112, Springer-Verlag, New York, 1995.

[19] C. M. Marcus and R. M. Westervelt, *Stability of analog networks with delay*, Phys. Rev. A, 39 (1989), pp. 347–359.

[20] L. Olien and J. Belair, *Bifurcations, stability, and monotonicity properties of a delayed neural network model*, Phys. D, 102 (1997), pp. 349–363.

[21] K. Pakdaman, C. P. Malta, C. Grotta-Ragazzo, O. Arino, and J.-F. Vibert, *Transient oscillations in continuous-time excitatory ring neural networks with delay*, Phys. Rev. E, 55 (1997), pp. 3234–3248.

[22] D. R. Reddy, A. Sen, and G. Johnston, *Time delay induced death in coupled limit cycle oscillators*, Phys. Rev. Lett., 80 (1998), pp. 5109–5112.

[23] T. Roska, C. Wu, and L. Chua, *Stability of cellular neural networks with dominant nonlinear and delay-type templates*, IEEE Trans. Circuits Systems I, 40 (1993), pp. 270–272.

[24] H. G. Schuster, ed., *Nonlinear Dynamics and Neuronal Networks*, Weinheim:VCH, New York, 1991.

[25] L. P. Shayer,*Analysis of a System of Two Coupled Neurons with Two Time Delays*, Master's thesis, University of Waterloo, ON, Canada, 1998.

[26] G. Stépán, *Retarded Dynamical Systems*, Pitman Res. Notes Math. Ser. 210, Longman Group, Essex, UK, 1989.
[27] W. Wischert, A. Wunderlin, A. Pelster, M. Olivier, and J. Groslambert, *Delay-induced instabilities in nonlinear feedback systems*, Phys. Rev. E, 49 (1994), pp. 203–219.
[28] H. Ye, A. Michel, and K. Wang, *Global stability and local stability of Hopfield neural networks with delays*, Phys. Rev. E, 50 (1994), pp. 4206–4213.
[29] H. Ye, A. Michel, and K. Wang, *Qualitative analysis of Cohen-Grossberg neural networks with multiple delays*, Phys. Rev. E, 51 (1995), pp. 2611–2618.